from patients before treatment and at Weeks 1, 4, 8, 12, 24, and 48 during the therapy. Peripheral blood mononuclear cells (PBMCs) were collected by density-gradient centrifugation on a Ficoll–Hypaque cushion. After viable PBMCs had been counted, the cells were stained with combinations of various antibodies for phenotypic markers.

The following monoclonal antibodies were purchased from BD Biosciences (San Jose, CA): anti-lineagemarker (Lin; CD3 (clone SK7), CD14 (clone MφP9), CD16 (clone 3G8), CD19 (clone SJ25C1), CD20 (clone L27), and CD56 (clone NCAM16.2)), anti-CD4 (clone RPA-T4), anti-CD11c (clone B-ly6), anti-CD123 (clone 7G3), anti-CD3 (clone UCHT1), anti-CD45RO (clone UCHL1), anti-CD56 (clone B159), anti-HLA-DR (clone L243), anti-CCR4 (clone 1G1). Anti-CXCR3 (clone 49801) monoclonal antibody was purchased from R&D Systems (Minneapolis, MN). Staining was performed with FITC, PE, PerCP, and APC conjugated antibodies as described previously. The acquisitions and analyses of data were performed with FACSCalibur (BD Biosciences) and CellQuest software.

Blood dendritic cells were defined as Lin^- and $HLA\text{-}DR^+$ cells. Myeloid dendritic cells are Lin^-, $HLA\text{-}DR^+$, $CD11c^+$, $CD123^{low}$ cells, and plasmacytoid dendritic cells are Lin^-, $HLA\text{-}DR^+$, $CD11c^-$, and $CD123^{high}$ cells, respectively. Helper T cell subpopulations were defined by the pattern of CXCR3 and CCR4; Th1 cells are $CD4^+$, $CD45RO^+$, $CXCR3^+$, and Th2 cells are $CD4^+$, $CD45RO^+$, and $CCR4^+$, respectively. NK cells were defined as $CD3^-$, $CD56^+$ cells. The percentages of dendritic cell subsets and NK cells in PBMCs or Th1 and Th2 cells in $CD4^+$ T cells were determined by FACS. In order to examine the dynamics of dendritic cell subsets after initiation of the treatment, we used the ratio of frequencies at each time point to those before the therapy.

Allogeneic Mixed Leukocyte Reaction With Dendritic Cells

In some patients, we examined whether the allostimulatory ability of dendritic cells was related to the clinical outcomes. At the end of treatment and at Week 4 after completion of the treatment, monocyte-derived dendritic cells were generated from PBMC obtained from the patients according to methods reported previously [Romani et al., 1994]. As controls, monocyte-derived dendritic cells were generated simultaneously from healthy donors. As responder cells in mixed leukocyte reaction (MLR), naive $CD4^+$ T cells were isolated from PBMC of irrelevant healthy donors by using a naive $CD4^+$ T cell enrichment kit (Stemcell Technologies, Vancouver, BC). Allogeneic MLR with monocyte-derived dendritic cells was performed as reported previously [Kanto et al., 1999]. In order to compare the ability of monocyte-derived dendritic cells among patients, we determined the MLR ratio between patients and controls as counts per minute (cpm) of ^3H-thymidine incorporated into $CD4^+$ T cells at the T cell/dendritic cell ratio of 10/1.

Statistical Analyses

For statistical analysis, the non-parametric Mann–Whitney *U*-test was used between the groups. To analyze paired data, we used Wilcoxon's signed rank test. Differences of continuous variables between groups were compared by two-way ANOVA. *P*-values of less than 0.05 were considered to be statistically significant. These statistical analyses were performed with StatView software (Cary, NC).

RESULTS

Outcome of the PEG-IFNα and Ribavirin Therapy

Among the 32 patients who received PEG-IFNα2b and ribavirin combination therapy, 25 completed the therapy while 7 patients dropped out due to various adverse effects. Among the 25 patients who completed the therapy, 11 (44%) achieved sustained virological response, 11 (44%) showed transient response, and 3 (12%) showed no response (Table I). There was no difference in the baseline clinical parameters among these groups (Table I). With regard to HCV RNA at Week 12 in patients who completed the therapy, 11 were negative for HCV RNA (early responders), while the remaining 14 were not. Among 11 patients with early response, 7 were sustained virological responders and 4 were transient responders. Among 14 patients who were positive for serum HCV RNA at Week 12, 4 patients achieved sustained virological response, 7 showed transient response, and 3 showed no response. Details of the therapeutic response in the current study are shown in Figure 1.

TABLE I. Baseline Clinical Characteristics of the Patients

	All patients	SVR	TR	NR
Age[a]	50.0 ± 10.9	46.7 ± 12.4	54.1 ± 8.9	46.7 ± 9.3
Sex (M/F)	20/5	9/2	8/3	3/0
ALT (IU/l)[a]	99.3 ± 47.8	97.5 ± 50.9	103 ± 51.3	94.0 ± 34.6
HCV RNA (kilo copies/ml)[a]	3146 ± 2675	3685 ± 3023	2743 ± 2338	2647 ± 3163
Activity (minimal/mild/moderate)	7/7/11	5/3/3	1/4/6	1/0/2
Fibrosis (mild/moderate/severe)	11/12/2	6/5/0	3/7/1	2/0/1

ALT, alanine aminotransferase.
Histological activity and fibrosis were assessed according to the classification proposed by Desmet.
[a]Mean ± SD.

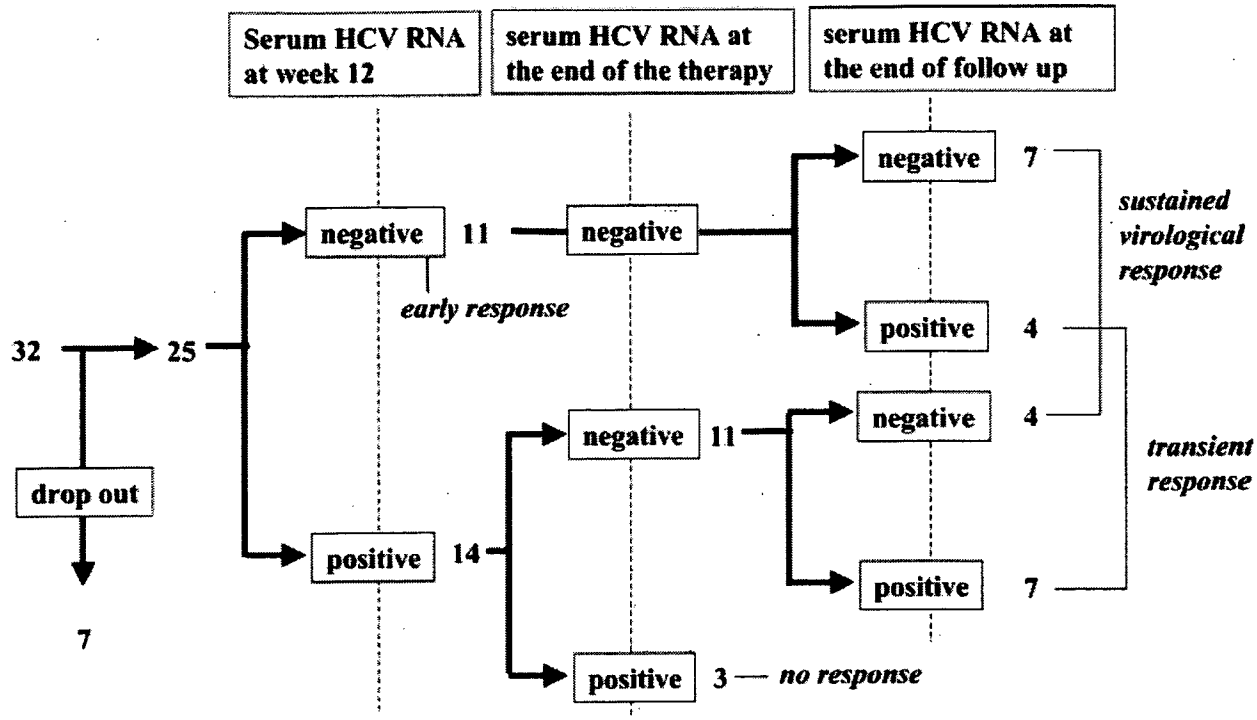

Fig. 1. Detailed outcomes of chronic hepatitis C patients treated with 48-week PEG-IFNα2b and ribavirin combination therapy. Thirty-two patients received the therapy, but seven dropped out due to various adverse effects. Among the 25 who completed the therapy, 11 achieved sustained virological response, 11 were transient responders, and 3 were non-responders. The early responders were defined as those who showed a reduction in HCV RNA quantity to an undetectable level by qualitative PCR at Week 12 of the therapy. According to this criterion, 11 patients were early responders and were further categorized into 7 sustained virological response (sustained virological responders with early response) and 4 transient response (transient responders with early response). Of the other 14 patients who were not early responders, 4 were sustained virological responders, 7 were transient responders, and 3 were non-responders.

Non-Sustained Virological Responders Had a Lower MLR Ratio Than Sustained Virological Responders

In order to clarify whether the frequency and function of immune cells are involved in the outcomes of the combination therapy, these parameters were compared between sustained virological responders and non-sustained virological responders, including transient responders and no responders. The pretreatment percentages of myeloid dendritic cells, plasmacytoid dendritic cells, NK cells, Th1, and Th2 were not different between the sustained virological responders and non-sustained virological responders (Fig. 2A). As for the changes of dendritic cell subsets during the therapy, frequencies of both plasmacytoid dendritic cells and myeloid dendritic cells at each time point did not differ between sustained virological responders and non-sustained virological responders (Fig. 2B,C). The percentages of NK cells in non-sustained virological responders tended to be higher than those in sustained virological responders from Weeks 4–48, which did not reach statistical significance ($P = 0.0533$ ANOVA) (Fig. 2F). The frequencies of Th1 and Th2 did not differ between these two groups (Fig. 2G,H). As for dendritic cell function, dendritic cells from the non-sustained virological responders showed a lower MLR ratio than those from the sustained virological responders at the end ($P < 0.01$) and at 4 weeks after the completion of therapy ($P < 0.005$) (Fig. 3). These results show that lesser ability of dendritic cells at the end of treatment may be related to non-sustained virological response.

Transient Responders Had a Lower MLR Ratio in Dendritic Cell Function Than Sustained Virological Responders in the Course of Combination Therapy

In order to elucidate if the above-mentioned immunological markers are related to virological relapse, a

Fig. 2. Pretreatment frequency of blood cells and its changes during 48-week PEG-IFNα2b and ribavirin therapy in sustained virological responders and non-sustained virological responders. Frequencies of myeloid dendritic cells, plasmacytoid dendritic cells, NK cells, Th1 cells, and Th2 cells in the patients before the treatment (**A**), during the combination therapy (**B**, **C**, **F**–**H**) and the ratios of myeloid dendritic cell or plasmacytoid dendritic cell frequency (**D**, **E**) were determined as described in Materials and Methods, which were compared between sustained virological responders and non-sustained virological responders. Black bars (A) or closed triangles (B–H) depict sustained virological responders and white bars (A) or closed circles (B–H) depict non-sustained virological responders. The results are expressed as the mean ± SEM of 11 sustained virological responders and 14 non-sustained virological responders. PBMC, peripheral blood mononuclear cells; NK, natural killer.

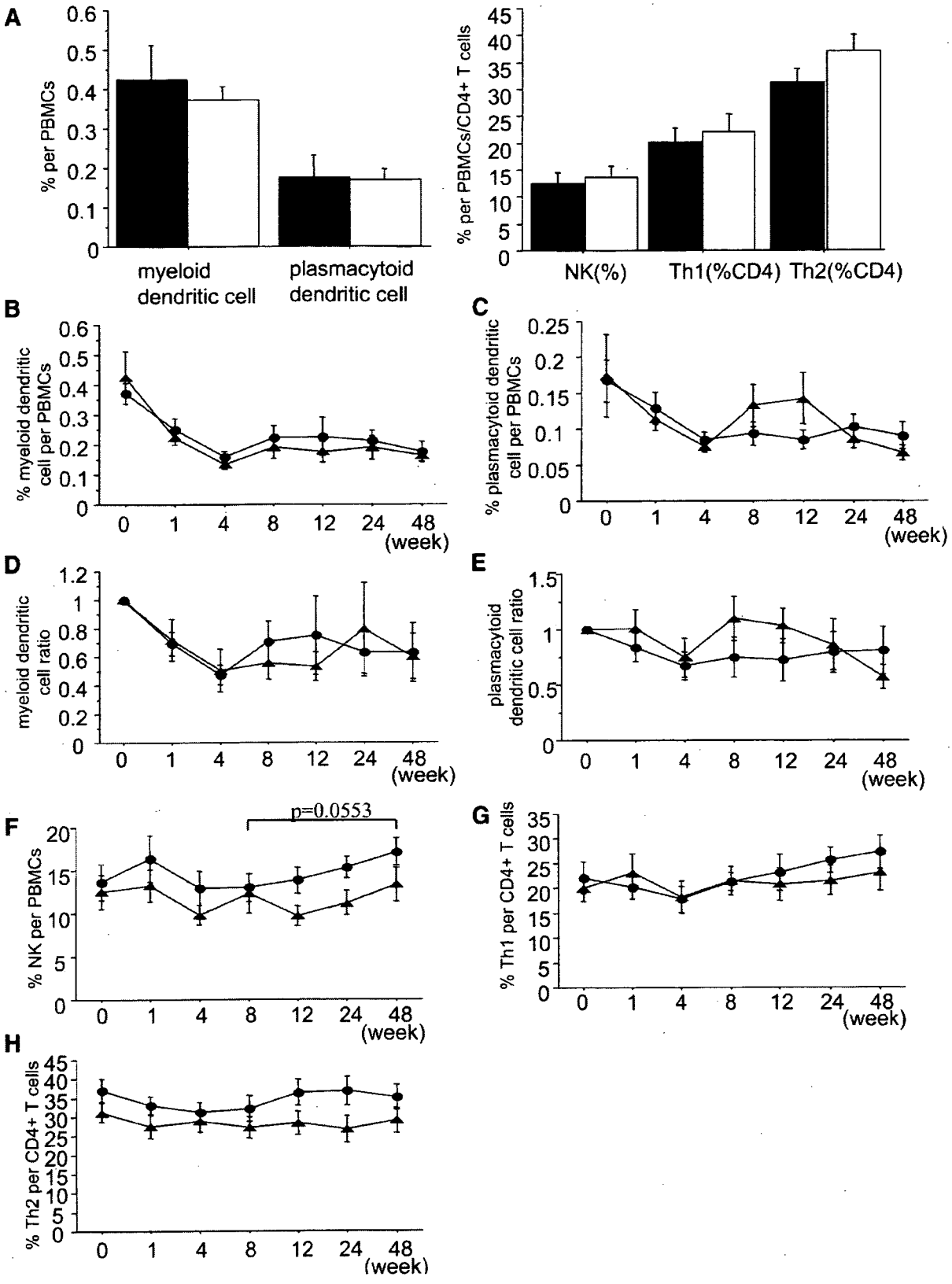
A
% per PBMCs
myeloid dendritic cell
plasmacytoid dendritic cell
% per PBMCs/CD4+ T cells
NK(%)
Th1(%CD4)
Th2(%CD4)
B
% myeloid dendritic cell per PBMCs
C
% plasmacytoid dendritic cell per PBMCs
D
myeloid dendritic cell ratio
E
plasmacytoid dendritic cell ratio
F
% NK per PBMCs
p=0.0553
G
% Th1 per CD4+ T cells
H
% Th2 per CD4+ T cells
0 1 4 8 12 24 48
(week)

Fig. 2.

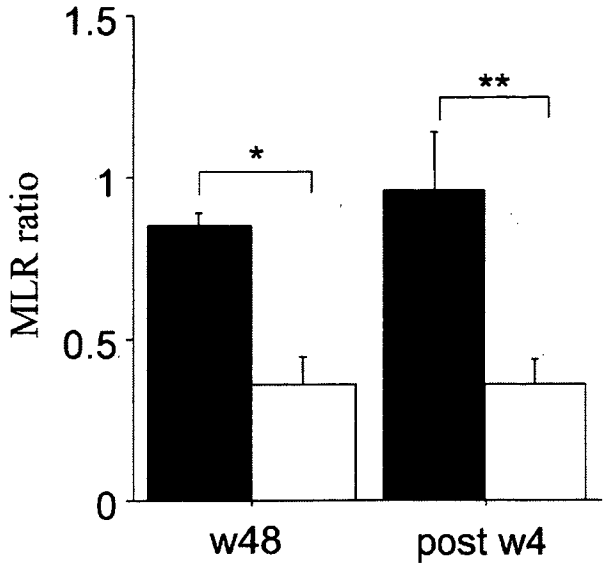

Fig. 3. Allostimulatory activity of dendritic cells in patients who underwent 48-week PEG-IFNα2b and ribavirin therapy in sustained virological responders and non-sustained virological responders. At the end of treatment (Week 48) and at Week 4 after completion of the treatment, monocyte-derived dendritic cells were generated from the patients or healthy donors and their allostimulatory capacity was evaluated as described in Materials and Methods. The MLR ratio between patients and controls was determined from the counts per minute (cpm) of ^{3}H-thymidine incorporated into CD4$^+$ T cells at T cell/dendritic cell ratio of 10/1. The results are expressed as the mean ± SEM of 11 sustained virological responders and 14 non-sustained virological responders. Black bars indicate sustained virological responders and white bars indicate non-sustained virological responders. *$P < 0.01$, **$P < 0.005$.

comparison was undertaken between sustained virological responders and transient responders. The pretreatment percentages of myeloid dendritic cells, plasmacytoid dendritic cells, NK cells, Th1, and Th2 were not different between the sustained virological responders and transient responders (Fig. 4A).

The percentages of myeloid dendritic cells and plasmacytoid dendritic cells were not different between the sustained virological responders and transient responders at each time point (Fig. 4B,C). The transient responders tended to show a lower plasmacytoid dendritic cell ratio than sustained virological responders from Weeks 1–12 ($P = 0.0553$, ANOVA) (Fig. 4E), suggesting that plasmacytoid dendritic cell is likely to decrease in the early phase in transient responders whereas those in sustained virological responders tend to be maintained. By contrast, no difference was observed in the myeloid dendritic cell ratio between the groups (Fig. 4D). The percentages of NK cells in transient responders were significantly higher than those in sustained virological responders from Weeks 8–48 ($P < 0.05$) (Fig. 4F). The frequencies of Th1 or Th2 at each point during therapy did not differ between the sustained virological responders and transient responders (Fig. 4G,H).

With regard to the dendritic cell function, the transient responders showed a lower MLR ratio than the sustained virological responders from Weeks 4–48 after the end of the therapy ($P < 0.05$) (Fig. 5). These results suggest that sustained impairment of dendritic cell function at the end and after the treatment may be related to the virological relapse after cessation of the therapy.

Early-Phase Decline of Plasmacytoid Dendritic Cell Frequency and Sustained Impairment of Dendritic Cell Ability Are Related to Transient Response in the Combination Therapy Even in Patients Who Lost Serum HCV RNA at Week 12 of the Treatment

In order to estimate more precisely the involvement of immunological markers in the outcomes of the combination therapy, we examined the above-mentioned parameters in patients who attained negative serum HCV RNA at Week 12 (early response group), as they were considered to be comparable with respect to the virological response to the therapy. Among 11 patients who were clear of serum HCV at Week 12, 7 were categorized into sustained virological response (sustained virological responders with early response) and the remaining 4 into transient response (transient responders with early response) (Fig. 1). Among patients with early response, the pretreatment percentages of myeloid dendritic cells, plasmacytoid dendritic cells, Th1, Th2, and NK cells (Fig. 6A) and those at any points during the therapy did not differ between sustained virological responders and transient responders (Fig. 6B,C,F–H). The plasmacytoid dendritic cell ratios in transient responders were lower than those in sustained virological responders from Weeks 1–12 ($P < 0.05$, ANOVA) (Fig. 6E), whereas the myeloid dendritic cell ratio did not differ between the groups (Fig. 6D).

As for MLR, dendritic cells from the transient responders showed a lower MLR ratio than those from the sustained virological responders at the end and at 4 weeks after the completion of therapy (Fig. 7) ($P < 0.001$).

DISCUSSION

In the PEG-IFNα and ribavirin therapy for chronic hepatitis C, viral and host factors are critically involved in the efficacy of treatment. As for viral factors, HCV

Fig. 4. Pretreatment frequency of blood cells and its changes during 48-week PEG-IFNα2b and ribavirin therapy in sustained virological responders and transient responders. Frequencies of myeloid dendritic cells, plasmacytoid dendritic cells, NK cells, Th1 cells, and Th2 cells in the patients before the treatment (**A**), during the combination therapy (**B, C, F–H**), and the ratios of myeloid dendritic cell or plasmacytoid dendritic cell frequency (**D, E**) were determined as described in Materials and Methods, which were compared between sustained virological responders and transient responders ones. Black bars (A) or closed triangles (B–H) depict sustained virological responders and white bars (A) or closed circles (B–H) depict transient responders. The results are expressed as the mean ± SEM of 11 sustained virological responders and 11 transient responders. PBMC, NK are shown in Figure 2. *$P < 0.05$ (sustained virological responders vs. transient responders).

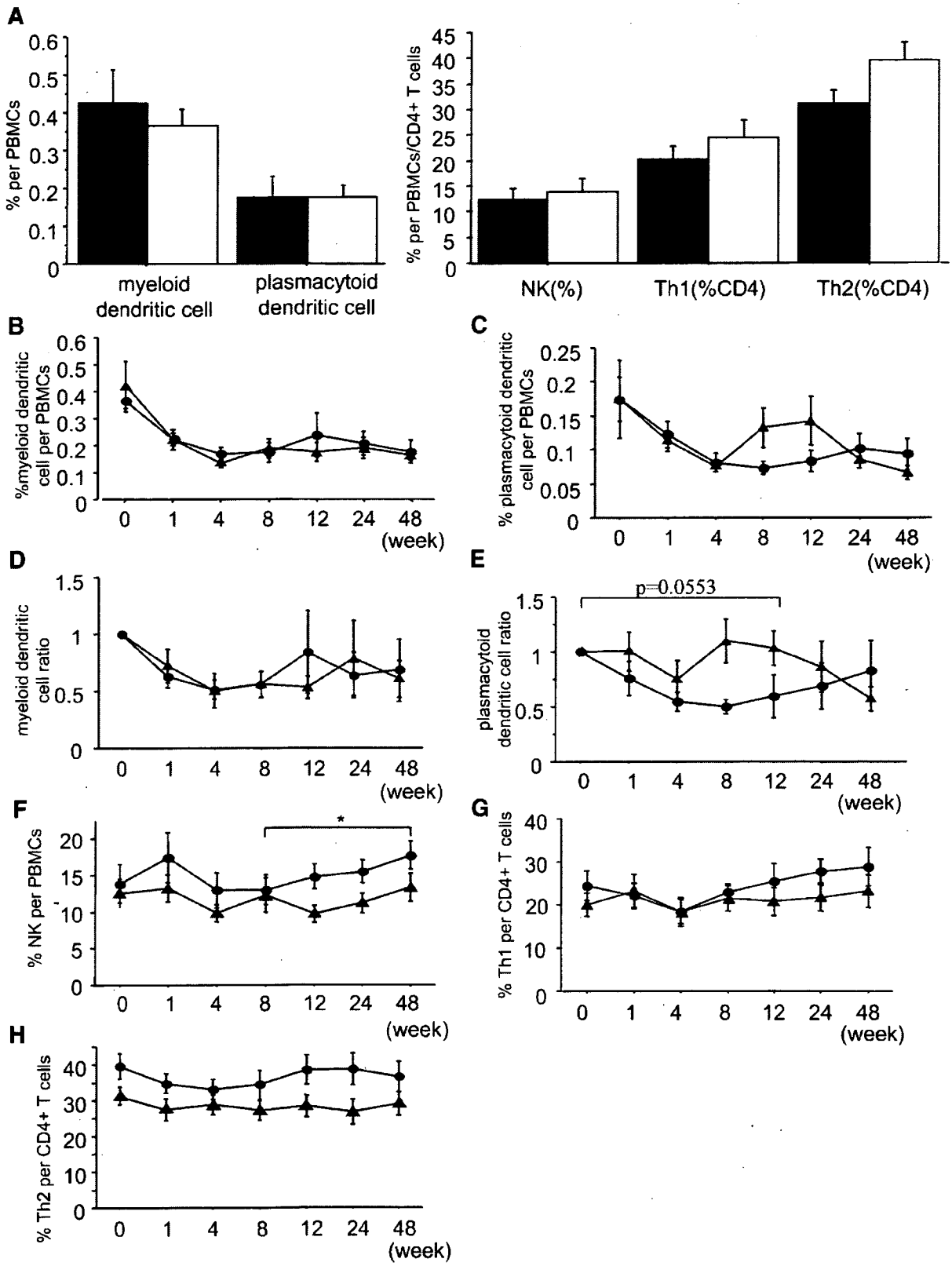
A
% per PBMCs
myeloid dendritic cell
plasmacytoid dendritic cell
% per PBMCs/CD4+ T cells
NK(%)
Th1(%CD4)
Th2(%CD4)
B
%myeloid dendritic cell per PBMCs
(week)
C
% plasmacytoid dendritic cell per PBMCs
(week)
D
myeloid dendritic cell ratio
(week)
E
p=0.0553
plasmacytoid dendritic cell ratio
(week)
F
*
% NK per PBMCs
(week)
G
% Th1 per CD4+ T cells
(week)
H
% Th2 per CD4+ T cells
(week)

Fig. 4.

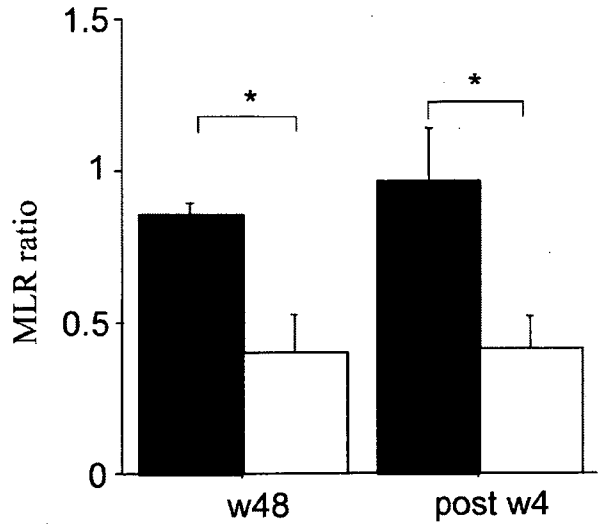

Fig. 5. Allostimulatory activity of dendritic cells in patients who underwent 48-week PEG-IFNα2b and ribavirin therapy in sustained virological responders and transient responders. At the end of treatment (Week 48) and at Week 4 after completion of the treatment, monocyte-derived dendritic cells were generated from the patients or healthy donors and their allostimulatory capacity was evaluated as described in Materials and Methods. The MLR ratio between patients and controls was determined as the same as Figure 3. The results are expressed as the mean ± SEM of 11 sustained virological responders and 11 transient responders. Black bars indicate sustained virological responders and white bars indicate transient responders. *$P < 0.05$.

genotypes and baseline HCV RNA titers are major determinants dictating therapeutic outcomes. In addition, failure of rapid decline in serum HCV RNA from the beginning of the treatment, i.e., non-early virological response, has been used as a negative predictor for sustained virological response. Alternatively, the enhancement of immunity has been implicated to play a key role in the successful responses in PEG-IFNα and ribavirin therapy. However, it is yet to be determined which parameters are practically feasible for the assessment of treatment-induced immune responses correlating with therapeutic efficacy.

In the present study, it was determined whether the frequencies of dendritic cells, NK cells, Th1 and Th2 cells, as well as dendritic cell function in patients are related to the outcome of the PEG-IFNα and ribavirin therapy. By comparing these markers in the course of the treatment between sustained virological responders and non-sustained virological responders, it was demonstrated that non-sustained virological responders showed impaired dendritic cell function in MLR than sustained virological responders. When the analyses were extended to comparison between sustained virological responders and transient responders, transient responders exhibited (1) lower plasmacytoid dendritic cell ratio, (2) higher NK cell frequency, and (3) impaired dendritic cell function than sustained virological responders. Of particular interest were the findings of a lower plasmacytoid dendritic cell ratio as well as lower MLR even in transient responders with early response compared to sustained virological responders with early response. Since patients with early response are defined as those who showed negative serum HCV RNA at Week 12, they are considered to be similar in virological response to the combination therapy. Thus, such parameters could serve as immunological markers for virological relapse, presumably being independent of the early virological response.

In general, homeostasis of blood cell number is regulated by their life span and their recruitment from the bone marrow to circulating blood. A reduction of blood cell numbers is frequently observed in patients who are treated with PEG-IFNα and ribavirin combination therapy, which may be due to bone marrow suppression, enhancement of cellular apoptosis, or alteration of localization. However, the dynamics of dendritic cell subsets or NK cells under combination therapy is yet to be clarified. Some investigators have reported that the frequency or the absolute number of blood dendritic cell is dynamically changed by various stresses, such as infection [Hotchkiss et al., 2002] or surgery [Ho et al., 2001]. The present study showed that reduction of plasmacytoid dendritic cells after the introduction of combination therapy is much greater in the transient responders than in the sustained virological responders. IFNα is reported to act as a regulatory factor on $CD11c^-$ dendritic cells to sustain their viability and to inhibit gaining the ability to stimulate Th2 development [Ito et al., 2001]. Thus, patients who respond well to IFNα, as demonstrated by better plasmacytoid dendritic cell survival during the treatment, are likely to have better chances to eradicate HCV. Limited information is available about the factors influencing the number of NK cells. In chronic HCV infection, it has been reported that the progression of liver disease is associated with a decrease of peripheral as well as liver-residing NK cells [Kawarabayashi et al., 2000]. It is plausible that the lower frequency of peripheral NK cells in the sustained virological responders compared to the transient responders, as shown in this study, may be related to the accumulation of NK cells in the liver, where they presumably produce IFNγ to suppress HCV replication. Further study is needed to disclose the reasons for the dynamics of these cells being related to the virological response in the combination therapy.

Fig. 6. Pretreatment frequency of blood cells and changes during 48-week PEG-IFNα2b and ribavirin therapy in patients who showed negative serum HCV RNA at Week 12 of the therapy. Frequencies of myeloid dendritic cells, plasmacytoid dendritic cells, NK cells, Th1 cells, and Th2 cells in the patients before the treatment (**A**), during the combination therapy (**B**, **C**, **F–H**) and the ratios of myeloid dendritic cell or plasmacytoid dendritic cell frequency (**D**, **E**) were determined as described in Materials and Methods, which were compared between sustained virological responders and transient responders ones. Black bars (A) or closed triangles (B–H) depict sustained virological responders and white bars (A) or closed circles (B–H) depict transient responders. The results are expressed as the mean±SEM of seven sustained virological responders with early response and four transient responders with early response. PBMC, NK are shown in Figure 2. *$P < 0.05$ (sustained virological responders vs. transient responders).

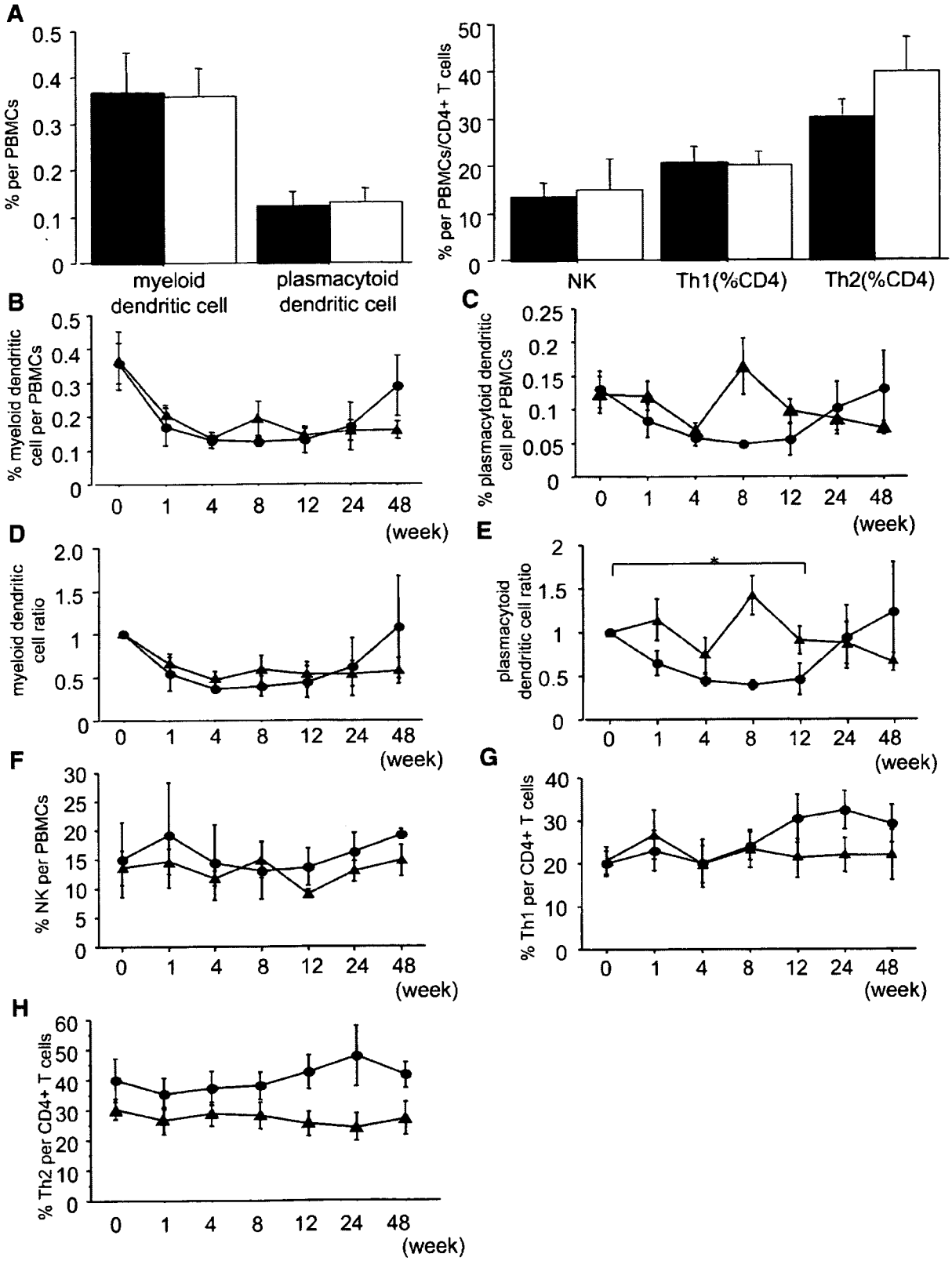
A
% per PBMCs
myeloid dendritic cell
plasmacytoid dendritic cell
% per PBMCs/CD4+ T cells
NK
Th1(%CD4)
Th2(%CD4)
B
% myeloid dendritic cell per PBMCs
C
% plasmacytoid dendritic cell per PBMCs
D
myeloid dendritic cell ratio
E
plasmacytoid dendritic cell ratio
F
% NK per PBMCs
G
% Th1 per CD4+ T cells
H
% Th2 per CD4+ T cells
(week)

Fig. 6.

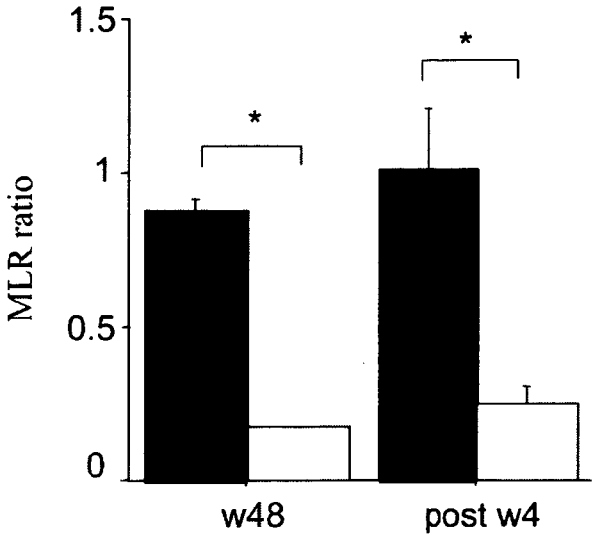

Fig. 7. Allostimulatory activity of dendritic cells in the patients who underwent 48-week PEG-IFNα2b and ribavirin therapy in patients who showed negative serum HCV RNA at Week 12 of the therapy. At the end of treatment (Week 48) and at Week 4 after the completion of the treatment, monocyte-derived dendritic cells were generated from the patients or healthy donors and their allostimulatory capacity was evaluated as described in Materials and Methods. The MLR ratio between patients and controls was determined as the same as Figure 3. The results are expressed as the mean ± SEM of seven sustained virological responders with early response and four transient responders with early response. Black bars indicate sustained virological responders and white bars indicate transient responders, respectively. *$P < 0.05$.

In the present study, non-sustained virological responders or transient responders showed a lesser capacity for dendritic cell function than sustained virological responders at the end and after cessation of the therapy. Even in the patients who lost serum HCV RNA at Week 12, the dendritic cell function was lower in transient responders than sustained virological responders. One of the mechanisms of impaired dendritic cell function in non-sustained virological responders or transient responders may be residual HCV both in serum and in cells. It is reported that the relapse rate was higher in the patients who were positive for HCV RNA by sensitive transcription-mediated amplification (TMA) at the end of combination therapy than those who were negative for it, even when they were negative for HCV RNA by conventional PCR [Gerotto et al., 2006]. Other investigators have shown that residual HCV is detectable by means of sensitive PCR in blood cells from patients who cleared HCV from the serum by IFNα and ribavirin combination therapy [Pham et al., 2004], supporting the possibility that blood cells are reservoirs of HCV replication. Taking these findings into consideration, it is conceivable that a small quantity of HCV might exist in the blood cells in some transient responders. Since direct HCV infection of monocytes or blood dendritic cells is considered to be one of the mechanisms of the functional impairment of dendritic cell [Navas et al., 2002; Goutagny et al., 2003; Ducoulombier et al., 2004], persistent HCV may delay the restoration of dendritic cell function in non-sustained virological responders or transient responders compared to sustained virological responders.

In summary, it was shown that the frequencies of plasmacytoid dendritic cells or NK cells and dendritic cell function might be related to the outcomes of the combination therapy. Since the present study was performed with a relatively small number of patients, a greater number of patients should be examined in order to validate the feasibility of using these as immunological markers of relapse. The prediction of virological non-response or relapse during therapy can help improve the clinical outcomes of treated patients, as prolongation of combination therapy offers potential relapsers a better chance of sustained virological response by suppressing HCV reappearance.

REFERENCES

Alter HJ, Purcell RH, Shih JW, Melpolder JC, Houghton M, Choo QL, Kuo G. 1989. Detection of antibody to hepatitis C virus in prospectively followed transfusion recipients with acute and chronic non-A, non-B hepatitis. N Engl J Med 321:1494–1500.

Auffermann-Gretzinger S, Keeffe EB, Levy S. 2001. Impaired dendritic cell maturation in patients with chronic, but not resolved, hepatitis C virus infection. Blood 97:3171–3176.

Berg T, von Wagner M, Nasser S, Sarrazin C, Heintges T, Gerlach T, Buggisch P, Goeser T, Räsenack J, Pape GR, Schmidt WE, Kallinowski B, Klinker H, Spengler U, Martus P, Alshuth U, Zeuzem S. 2006. Extended treatment duration for hepatitis C virus type 1: Comparing 48 versus 72 weeks of peginterferon-alfa-2a plus ribavirin. Gastroenterology 130:1086–1097.

Davis GL, Wong JB, McHutchison JG, Manns MP, Harvey J, Albrecht J. 2003. Early virologic response to treatment with peginterferon alfa-2b plus ribavirin in patients with chronic hepatitis C. Hepatology 38:645–652.

Desmet VJ, Gerber M, Hoofnagle JH, Manns M, Scheuer PJ. 1994. Classification of chronic hepatitis: Diagnosis, grading and staging. Hepatology 19:1513–1520.

Ducoulombier D, Roque-Afonso AM, Di Liberto G, Penin F, Kara R, Richard Y, Dussaix E, Feray C. 2004. Frequent compartmentalization of hepatitis C virus variants in circulating B cells and monocytes. Hepatology 39:817–825.

Ferenci P. 2004. Predicting the therapeutic response in patients with chronic hepatitis C: The role of viral kinetic studies. J Antimicrob Chemother 53:15–18.

Ferenci P, Fried MW, Shiffman ML, Smith CI, Marinos G, Goncales FL Jr, Haussinger D, Diago M, Carosi G, Dhumeaux D, Craxi A, Chaneac M, Reddy KR. 2005. Predicting sustained virological responses in chronic hepatitis C patients treated with peginterferon alfa-2a (40 KD)/ribavirin. J Hepatol 43:425–433.

Fried MW, Shiffman ML, Reddy KR, Smith C, Marinos G, Goncales FL Jr, Haussinger D, Diago M, Carosi G, Dhumeaux D, Craxi A, Lin A, Hoffman J, Yu J. 2002. Peginterferon alfa-2a plus ribavirin for chronic hepatitis C virus infection. N Engl J Med 347:975–982.

Gerotto M, Dal Pero F, Bortoletto G, Ferrari A, Pistis R, Sebastiani G, Fagiuoli S, Realdon S, Alberti A. 2006. Hepatitis C minimal residual viremia (MRV) detected by TMA at the end of Peg-IFN plus ribavirin therapy predicts post-treatment relapse. J Hepatol 44: 83–87.

Goutagny N, Fatmi A, De Ledinghen V, Penin F, Couzigou P, Inchauspe G, Bain C. 2003. Evidence of viral replication in circulating dendritic cells during hepatitis C virus infection. J Infect Dis 187: 1951–1958.

Hayashi N, Takehara T. 2006. Antiviral therapy for chronic hepatitis C: Past, present, and future. J Gastroenterol 41:17–27.

Ho CS, Lopez JA, Vuckovic S, Pyke CM, Hockey RL, Hart DN. 2001. Surgical and physical stress increases circulating blood dendritic cell counts independently of monocyte counts. Blood 98:140–145.

Hotchkiss RS, Tinsley KW, Swanson PE, Grayson MH, Osborne DF, Wagner TH, Cobb JP, Coopersmith C, Karl IE. 2002. Depletion of

dendritic cells, but not macrophages, in patients with sepsis. J Immunol 168:2493–2500.

Ito T, Amakawa R, Inaba M, Ikehara S, Inaba K, Fukuhara S. 2001. Differential regulation of human blood dendritic cell subsets by IFNs. J Immunol 166:2961–2969.

Jacobson IM, Gonzalez SA, Ahmed F, Lebovics E, Min AD, Bodenheimer HC Jr, Esposito SP, Brown RS Jr, Brau N, Klion FM, Tobias H, Bini EJ, Brodsky N, Cerulli MA, Aytaman A, Gardner PW, Geders JM, Spivack JE, Rahmin MG, Berman DH, Ehrlich J, Russo MW, Chait M, Rovner D, Edlin BR. 2005. A randomized trial of pegylated interferon alpha-2b plus ribavirin in the retreatment of chronic hepatitis C. Am J Gastroenterol 100:2453–2462.

Kamal SM, Fehr J, Roesler B, Peters T, Rasenack JW. 2002. Peginterferon alone or with ribavirin enhances HCV-specific CD4 T-helper 1 responses in patients with chronic hepatitis C. Gastroenterology 123:1070–1083.

Kanto T, Hayashi N, Takehara T, Tatsumi T, Kuzushita N, Ito A, Sasaki Y, Kasahara A, Hori M. 1999. Impaired allostimulatory capacity of peripheral blood dendritic cells recovered from hepatitis C virus-infected individuals. J Immunol 162:5584–5591.

Kawarabayashi N, Seki S, Hatsuse K, Ohkawa T, Koike Y, Aihara T, Habu Y, Nakagawa R, Ami K, Hiraide H, Mochizuki H. 2000. Decrease of CD56(+)T cells and natural killer cells in cirrhotic livers with hepatitis C may be involved in their susceptibility to hepatocellular carcinoma. Hepatology 32:962–969.

Manesis EK, Papaioannou C, Gioustozi A, Kafiri G, Koskinas J, Hadziyannis SJ. 1997. Biochemical and virological outcome of patients with chronic hepatitis C treated with interferon alfa-2b for 6 or 12 months: A 4-year follow-up of 211 patients. Hepatology 26:734–739.

Manns MP, McHutchison JG, Gordon SC, Rustgi VK, Shiffman M, Reindollar R, Goodman ZD, Koury K, Ling M, Albrecht JK. 2001. Peginterferon alfa-2b plus ribavirin compared with interferon alfa-2b plus ribavirin for initial treatment of chronic hepatitis C: A randomised trial. Lancet 358:958–965.

Nattermann J, Feldmann G, Ahlenstiel G, Langhans B, Sauerbruch T, Spengler U. 2006. Surface expression and cytolytic function of natural killer cell receptors is altered in chronic hepatitis C. Gut 55:869–877.

Navas MC, Fuchs A, Schvoerer E, Bohbot A, Aubertin AM, Stoll-Keller F. 2002. Dendritic cell susceptibility to hepatitis C virus genotype 1 infection. J Med Virol 67:152–161.

Pawlotsky JM, Bouvier-Alias M, Hezode C, Darthuy F, Remire J, Dhumeaux D. 2000. Standardization of hepatitis C virus RNA quantification. Hepatology 32:654–659.

Pham TN, MacParland SA, Mulrooney PM, Cooksley H, Naoumov NV, Michalak TI. 2004. Hepatitis C virus persistence after spontaneous or treatment-induced resolution of hepatitis C. J Virol 78:5867–5874.

Poynard T, Marcellin P, Lee SS, Niederau C, Minuk GS, Ideo G, Bain V, Heathcote J, Zeuzem S, Trepo C, Albrecht J. 1998. Randomised trial of interferon alpha2b plus ribavirin for 48 weeks or for 24 weeks versus interferon alpha2b plus placebo for 48 weeks for treatment of chronic infection with hepatitis C virus. International Hepatitis Interventional Therapy Group (IHIT). Lancet 352: 1426–1432.

Romani N, Gruner S, Brang D, Kampgen E, Lenz A, Trockenbacher B, Konwalinka G, Fritsch PO, Steinman RM, Schuler G. 1994. Proliferating dendritic cell progenitors in human blood. J Exp Med 180:83–93.

Rosen HR, Miner C, Sasaki AW, Lewinsohn DM, Conrad AJ, Bakke A, Bouwer HG, Hinrichs DJ. 2002. Frequencies of HCV-specific effector CD4+ T cells by flow cytometry: Correlation with clinical disease stages. Hepatology 35:190–198.

Seeff LB. 2002. Natural history of chronic hepatitis C. Hepatology 36: S35–S46.

Int. J. Cancer: 121, 878–883 (2007)

Synergistic antitumor effects of celecoxib with 5-fluorouracil depend on IFN-γ

Takanobu Irie[1], Masahiko Tsujii[1]*, Shingo Tsuji[1], Toshiyuki Yoshio[1], Shuji Ishii[1], Shinichiro Shinzaki[1], Satoshi Egawa[1], Yoshimi Kakiuchi[1], Tsutomu Nishida[1], Masakazu Yasumaru[1], Hideki Iijima[1], Hiroaki Murata[1], Tetsuo Takehara[1], Sunao Kawano[2] and Norio Hayashi[1]

[1]*Department of Gastroenterology and Hepatology, Osaka University Graduate School of Medicine, Osaka, Japan*
[2]*Department of Clinical Laboratory Science, Osaka University Graduate School of Medicine, Osaka, Japan*

Cyclooxygenase-2 (COX-2) inhibitors are effective chemopreventive agents against colorectal cancers. For treatment of advanced cancers, combination of COX-2 inhibitors and chemotherapy has been attempted, but the results are still controversial. In the present study, the effects of the COX-2 inhibitor celecoxib on the anticancer potential of chemotherapy, and its mechanisms of action were investigated in point of the angiogenesis, using an advanced cancer model in mice. BALB/c mice were inoculated with colon 26 cells. After the allograft grew up to 5 mm in diameter, the animals received celecoxib, 5FU, or a combination of 5FU and celecoxib (5FU/celecoxib). After 21-days of the treatment, 5FU/celecoxib significantly inhibited the tumor growth and the tumor vessel density compared with the other groups. Celecoxib, 5FU or 5FU/celecoxib significantly suppressed the VEGF content in tumor tissues. 5FU/celecoxib also enhanced IFN-γ levels in tumor tissue, which could be involved in the potent antitumor effects of 5FU/celecoxib. This hypothesis was proven, because in IFN-γ knockout (IFN-$\gamma^{-/-}$) mice, the inhibitory effects of 5FU/celecoxib on angiogenesis and tumor growth were significantly impaired compared with that in wild type mice. These results suggest that celecoxib enhances the antitumor effect of 5FU against an advanced colon cancer model by suppressing angiogenesis. In addition to VEGF, IFN-γ has pivotal roles in tumor suppression induced by celecoxib.

Key words: advanced colorectal cancer; COX-2; 5FU; IFN-γ; VEGF

Epidemiological studies suggest that long-term use of nonsteroidal anti-inflammatory drugs (NSAIDs) reduce the risk of colon cancer.[1] One of the targets of NSAIDs is cyclooxygenase (COX), a key enzyme in prostaglandin (PG) synthesis. COX-2, the inducible isozyme of COX, is highly expressed in a variety of cancers including colon, lung, prostate and stomach. Many reports have revealed that COX-2 is responsible for resistance to apoptosis, tumor growth, increased angiogenesis and enhanced invasion and metastasis.[2–4] COX-2 and PGE_2 enhance cell proliferation by promoting resistance to apoptosis, and activating EGFR and extra cellular signal-regulated kinase-2 (ERK-2),[5] insulin-like growth factor-I receptor (IGF-IR)[6] and hepatocyte growth factor (HGF).[7] COX-2 and PGE_2 also promote angiogenesis by stimulating the production of VEGF, bFGF and TGF-β.[8] We and others found that several COX-2 inhibitors significantly suppressed tumor growth provided treatment is started before,[6] or at the time of tumor inoculation.[9] Therefore, COX-2 inhibitors are thought to be promising chemopreventive agents against cancer.

Several preclinical studies have suggested that COX-2 inhibitors may enhance the effects of anticancer-agents.[10,11] In a clinical study, celecoxib enhanced effect of capecitabine.[12] In a phase II trial; however, rofecoxib did not appear to increase anti tumor activity of 5FU with leucovorin in metastatic colon cancer patients.[13] Therefore, the effects of COX-2 inhibitors in combination with chemotherapeutic agents against advanced cancer have not yet been elucidated in detail.

This study investigates whether celecoxib alone suppresses the growth of advanced cancer, and whether celecoxib in combination with 5-fluorouracil (5FU) enhances the tumoricidal effect of chemotherapy in mice. If celecoxib, with and without 5FU, is effective in tumor suppression, the second aim of the study is to explore putative mechanisms of how celecoxib influences the biology of the tumor. We paid particular attention to the influence of celecoxib and 5FU on the tumor microenvironment, *e.g.* angiogenesis, within the tumor.

Material and methods

Reagents

5FU was purchased from Nacalai Tesque, (Kyoto, Japan) and dissolved in phosphate buffered saline (PBS) at a concentration of 10 mg/ml. Celecoxib, a COX-2 inhibitor, was a kind gift from Pfizer Pharmaceuticals (New York, NY) and was dissolved in DMSO (100 mg/ml). A rat antibody against mouse CD31 (Platelet-Endothelial Cell Adhesion Molecule-1; PECAM-1) was purchased from HyCult biotechnology b.v. (Uden, Netherlands).

Cell culture

Colon 26 cells, a colon cancer cell line derived from BALB/c mice that express COX-2[6] were cultured in RPMI 1640 medium (Sigma Chemical, St. Louis, MO) supplemented with 10% FCS (JRH Biosciences, Lenexa, KS) and 1% antibiotics and antimycotics (Life Technologies, Grand Island, NY) in an atmosphere of 95% air and 5% CO_2 at 37°C.

In vivo *tumor growth*

All animal studies were conducted in accordance with the principles and procedures approved by the institutional committee for animal experiments. Male BALB/c mice aged 8 weeks were obtained from Japan SLC, (Hamamatsu, Japan). IFN-γ knockout (IFN-$\gamma^{-/-}$) mice were the kind gift of Dr. Yoichiro Iwakuma (The University of Tokyo, The Institute of Medical Science, Tokyo, Japan). All of the mice were maintained under specific pathogen-free conditions at the Center for Animal Experimentation, Osaka University Graduate School of Medicine. Regular laboratory food and tap water were freely available to the animals. The mice were inoculated subcutaneously with colon 26 tumor cells (1×10^7 cells). When the longest diameter of the tumor grew to more than 5 mm (day 0), the mice were randomized into one of 4 groups (9 animals/group) designated by treatment as control (untreated), celecoxib, 5FU and 5FU and celecoxib combined (5FU/celecoxib). Each reagent was administered by intra-peritoneal injection. Control group mice were intraperitone-

Abbreviations: 5FU, 5-fluorouracil; bFGF, basic fibroblast growth factor; COX-2, Cyclooxygenase-2; DMSO, dimethyl sulfoxide; EGFR, epidermal growth factor receptor; ELISA, enzyme linked immunosolvent assay; ERK-2, extra cellular signal-regulated kinase-2; HGF, hepatocyte growth factor; IFN-γ, interferon-gamma; IGF-IR, insulin-like growth factor-I receptor; IL-10, interleukin 10; IL-12, interleukin 12; NSAIDs, nonsteroidal anti-inflammatory drugs; PGE_2, prostaglandin E_2; TGF-β, transforming growth factor; VEGF, vascular endothelial growth factor;

***Correspondence to:** Department of Gastroenterology and Hepatology, Clinical Research Building (K1), Osaka University Graduate School of Medicine, 2-2 Yamadaoka, Suita, Osaka 565-0871, Japan.
Fax: +81-6-6879-3629. E-mail: mt@gh.med.osaka-u.ac.jp
Received 13 November 2006; Accepted after revision 16 February 2007
DOI 10.1002/ijc.22720
Published online 20 April 2007 in Wiley InterScience (www.interscience.wiley.com).

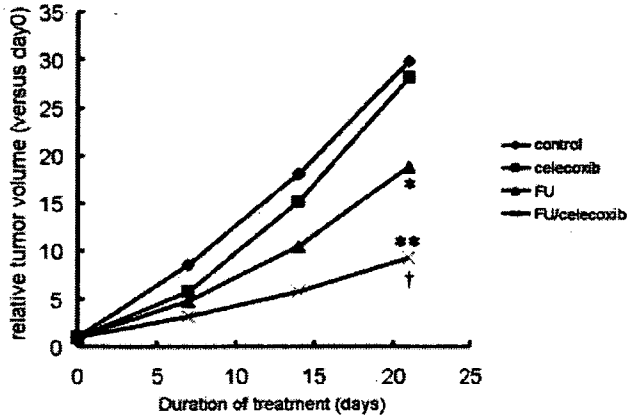

FIGURE 1 – The effect of celecoxib and 5FU on *in vivo* tumor growth. 1×10^7 colon 26 tumor cells were subcutaneously inoculated into an area on the backs of BALB/c mice. After the longest diameter of the tumor reached 5 mm or more, the mice were randomized to receive treatment with 5FU, celecoxib, 5FU and celecoxib, or no treatment. Data from each treatment group represent the mean ± SD (ratio *versus* day 0) of the results in 9 mice. $*p < 0.05$ and $**p < 0.0001$ *versus* control. $\dagger p < 0.01$ *versus* 5FU.

ally administered 1 ml of PBS and 20 µl of DMSO. Celecoxib group animals were treated similarly except that celecoxib (3 mg/kg body weight) rather than DMSO was administered every day, with PBS as described.[14] The 5FU group was treated with 5FU (20 mg/kg) and DMSO for 5 consecutive days a week as described,[15,16] and 5FU/celecoxib group was treated with both celecoxib (3 mg/kg) and 5FU (20 mg/kg) as aforementioned. During treatment, tumor volume was determined weekly by measuring the tumor's longest and shortest diameter, and volume calculated according to the following formula: volume (mm^3) = (the shortest diameter)^2 × (the longest diameter) × 0.5.[17] After 21 days, the mice were sacrificed by over anesthetization. The tumor was removed and used for immunofluorescent microscopic analysis, and ELISA assay.

Immunofluorescent microscopic analyses

Frozen tumor sections were cut into 5 µm thick slices and placed on slides. The slides were incubated with 3% normal rabbit serum in TBS with 0.25% Triton X-100 to block nonspecific binding, then incubated with rat anti-mouse CD31 antibody in 3% normal rabbit serum in TBS with 0.25% Triton X-100 overnight at 4°C. The negative control sections were incubated with 3% normal rabbit serum alone. After rinsing with TBS, the sections were incubated with secondary rhodamine conjugated chicken anti-rat antibody for 30 min at 37°C. Afterwards, the slides were

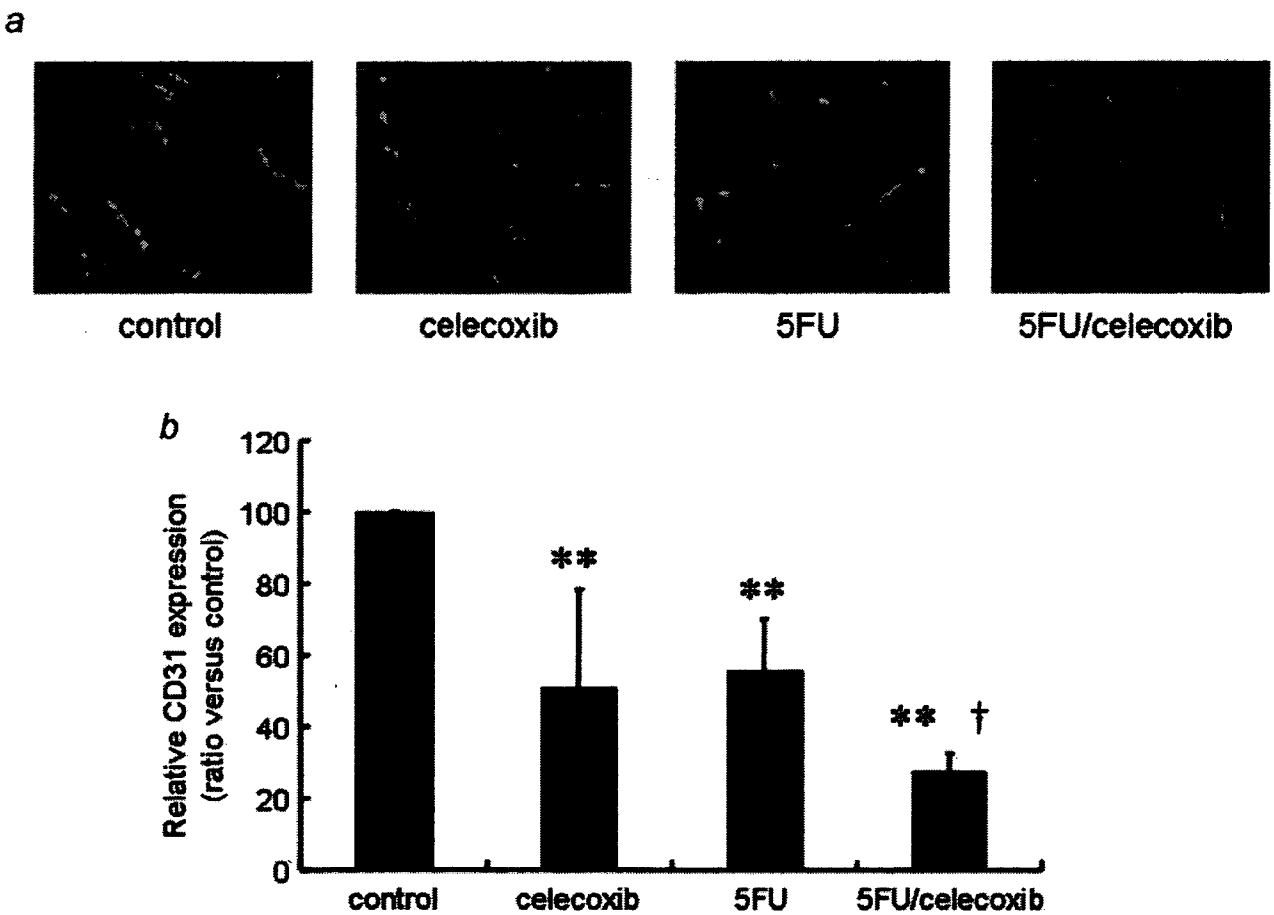

FIGURE 2 – The effects of celecoxib and 5FU on tumor angiogenesis. Tumor microvessel density was determined by CD31 (PEACAM-1) expression using immunofluorescent microscopic analyses. (*a*) Immunofluorescent image using anti-CD31 antibody. Original magnification was ×400. (*b*) Quantitative analysis of tumor angiogenesis. The CD31 expressing area per field was calculated by NIH Image processing and analysis software (NIH, Bethesda, MD). Data are shown as the mean ± SD (ratio versus non-treated control) of 4 mice in each group (percent versus control). $**p < 0.01$ *versus* control, $\dagger p < 0.01$ *versus* 5FU alone.

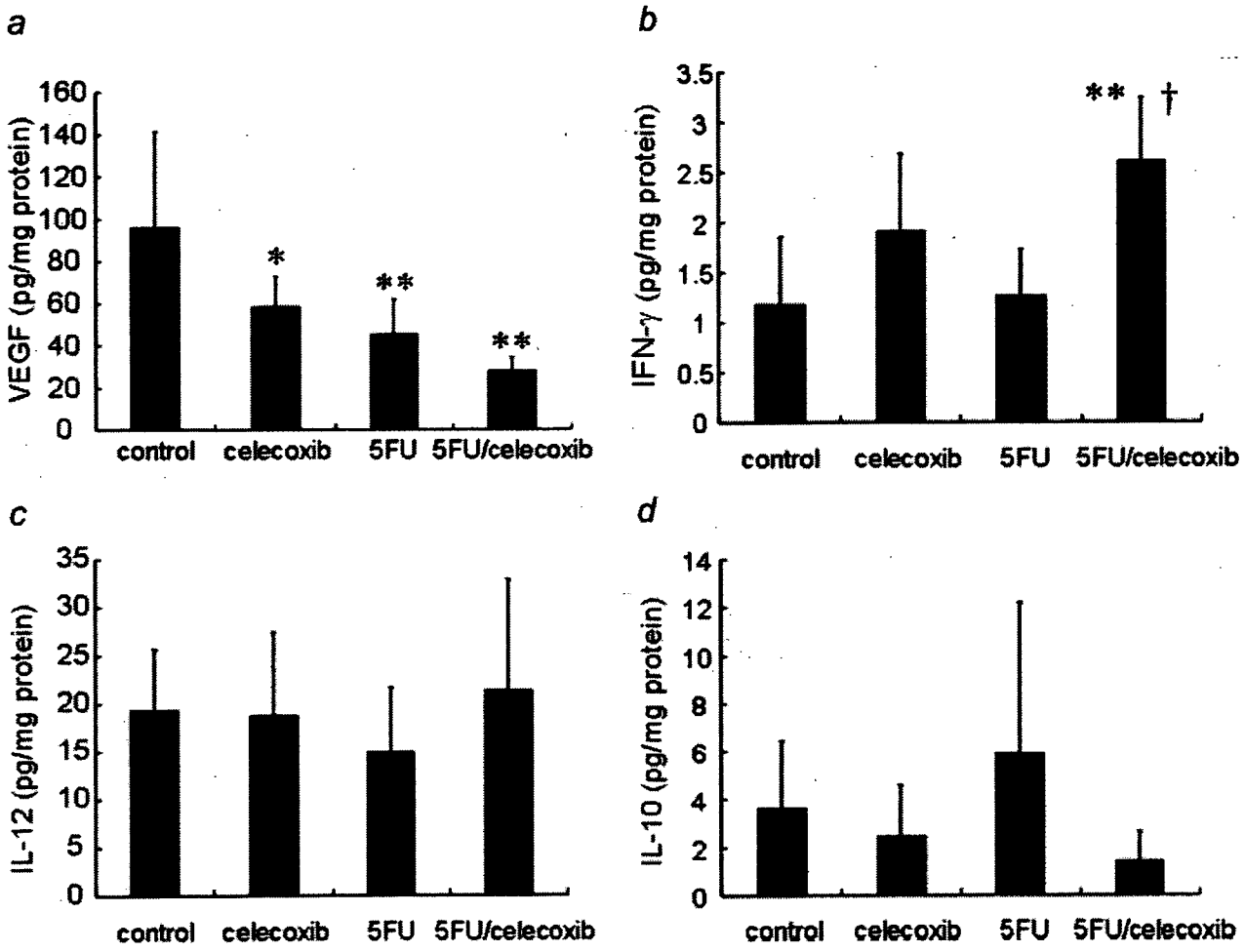

FIGURE 3 – The effect of celecoxib and 5FU on VEGF and cytokine levels in tumors. Tumors were homogenized as described in materials and methods. The concentration of VEGF and various cytokines in the tumors were measured by ELISA. (*a*) VEGF, (*b*) IFN-γ, (*c*) IL-12 and (*d*) IL-10 levels in the tumors are shown. Data are shown as the mean ± SD of 4 or 6 mice in each group (percentage of control). *$p < 0.05$ *versus* control. **$p < 0.01$ *versus* control. †$p < 0.01$ *versus* 5FU.

washed and mounted in antifade solution with DAPI (Vectashield, Vector, Burlingame, CA). Images were captured using a fluorescence microscope (Biozero BZ8000, Keyence, Osaka, Japan). To determine CD31 the signal area per field was measured with NIH Image software (NIH, Bethesda, MD) for image processing and analysis.

ELISA assay

The tumors were homogenized with a Polytron homogenizer (Kinematica AG, Littau, Switzerland) in a radioimmunoprecipitation assay buffer [1% Nonidet P-40, 0.5% sodium deoxycholate, 0.1% sodium dodecyl sulfate, 50 μg/ml aprotinin, 1 μg/ml leupeptin, 1 μg/ml pepstatin, 100 μg/ml phenylmethylsulfonyl fluoride, 1 mM sodium orthovanadate and 50 mM sodium fluoride in PBS (pH 7.4)]. The supernatant from centrifuged lysates were used to measure murine vascular endothelial growth factor (VEGF), IL-10, IL-12 and IFN-γ by ELISA assay kits (R&D systems, Abingdon, United Kingdom, for VEGF, IL-10 and IFN-γ, and BD Biosciences, San Jose, CA, for IL-12).

Statistical analysis

Statistically significant differences among data sets of multiple groups were analyzed using ANOVA followed by Fisher's protected least significant difference.

Results

Tumor growth

The effects of celecoxib, 5FU, and 5FU/celecoxib on the growth of tumors, which had grown to at least 5 mm in diameter, were investigated (Fig. 1). Celecoxib at the dose of 3 mg/kg did not significantly suppress the tumor growth compared with control. 5FU at the dose of 20 mg/kg significantly suppressed tumor growth compared with control ($p = 0.03$) or celecoxib alone ($p = 0.02$). Combination therapy with 5FU and celecoxib significantly reduced suppressed tumor growth compared with control ($p < 0.0001$) or either of the respective single agent treatment groups ($p < 0.0001$ versus celecoxib and $p = 0.004$ *versus* 5FU).

Tumor microvessel density

The CD31-positive microvessels developed in the cancer allografts in the untreated control animals. Celecoxib alone, 5FU alone or combination of 5FU and celecoxib decreased the tumor microvessel density compared with control. The combination of 5FU and celecoxib exerted the most significant suppression to the microvessel density in the tumor within the four study groups (Fig. 2).

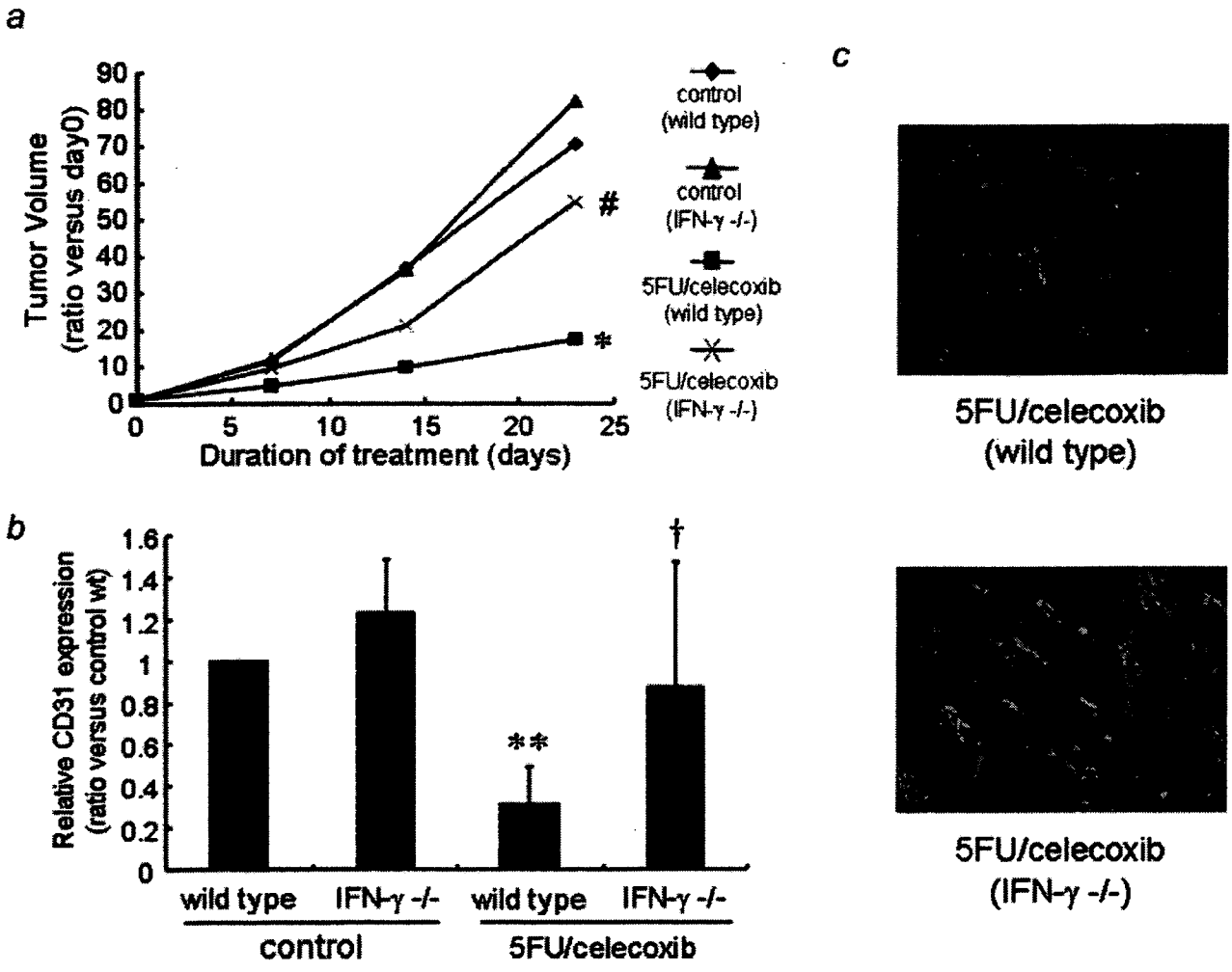

FIGURE 4 – The effect of combination therapy on tumor growth and angiogenesis in IFN-γ knockout (IFN-$\gamma^{-/-}$) mice. (*a*) Tumor growth. 1×10^7 colon 26 tumor cells were inoculated into wild type BALB/c mice or IFN-$\gamma^{-/-}$ mice. When the tumor's longest diameter reached 5 mm or more, the mice were randomized to treatment with 5FU and celecoxib, or no treatment. *$p < 0.05$ *versus* wild type, #$p < 0.05$ versus 5FU/celecoxib (wild type). Data are shown as the mean ± SD (ratio versus day 0) of 6 mice in each group. (*b–c*) CD31 expression. (*b*) Quantitative analysis of tumor angiogenesis. The CD31 expressing area per field was measured with NIH Image analyzing system software (NIH, Bethesda, MD). Data are shown as the mean ± SD (ratio *versus* wild type untreated control) of 4 mice in each group. **$p < 0.01$ *versus* control (wild type), †$p < 0.01$ *versus* FU/celecoxib (wild type). (*c*) Immunofluorescent pictures using anti-CD31 antibody. Original magnification was ×200.

VEGF and cytokine content in tumor tissue

Using tumor extract, the amounts of VEGF, IFN-γ, IL-12 and IL-10 in tumor tissue were determined (Fig. 3). Celecoxib, 5FU, and 5FU/celecoxib significantly reduced VEGF content (Fig. 3*a*). IFN-γ content in tumor tissue was significantly increased by 5FU/celecoxib-combined treatment (2.60 ± 0.63 pg/mg protein) compared with 5FU alone (1.25 ± 0.47) (Fig. 3*b*). There were not significant differences about the levels of IL-10 or IL-12 between treated and untreated groups (Figs. 3*c* and 3*d*).

Role of IFN-γ in antitumor effect enhanced by combined 5FU/celecoxib treatment

To investigate the role of increased IFN-γ levels in the enhanced antitumor effect of 5FU/celecoxib, the inhibitory effects of 5FU/celecoxib treatment on tumor growth in colon 26 cells inoculated IFN-$\gamma^{-/-}$ mice were determined and compared with those in wild type mice. At the end of treatment, the sizes of tumors in IFN-$\gamma^{-/-}$ mice treated with 5FU/celecoxib were significantly larger than those in wild type mice (Fig. 4*a*). These results indicated that the loss of host IFN-γ compromised the growth inhibitory effect of 5FU/celecoxib treatment.

The microvessel density in the tumors treated with 5FU/celecoxib in the IFN-$\gamma^{-/-}$ mice was significantly higher than that in the wild type mice (Figs. 4*b* and 4*c*), which also suggested that loss of host IFN-γ impaired the antiangiogenic effect of combined 5FU/celecoxib therapy.

Discussion

The present study shows that the combination of 5FU and celecoxib has greater tumoricidal activity than celecoxib or 5FU alone. The influence of celecoxib when combined with 5FU at doses higher than 20 mg/kg on drug-induced death in tumor-bearing mice have been reported elsewhere.[18] In the present study, significant adverse events were not observed in any group of mice at the 5FU dose of 20 mg/kg and the celecoxib dose of 3 mg/kg. Therefore, the results appear to reflect the features of these agents when they are most effective, and have the least side effects, although the most appropriate dosage remains to be investigated.

The present results clearly demonstrate synergistic effects of celecoxib in cancer chemotherapy using 5FU. Furthermore, the present study also investigated the mechanism whereby celecoxib, a COX-2 inhibitor, enhances the antitumor effects of 5FU. In particular, the effects of celecoxib and 5FU on the tumor microenvironments, namely tumor angiogenesis, VEGF, and several cytokines that might affect tumor angiogenesis, were explored. The results unexpectedly demonstrate that IFN-γ is involved in celecoxib-induced inhibition in tumor angiogenesis together with VEGF.

Tumor angiogenesis plays an important role in tumor promotion and progression.[19] We have shown that COX-2-derived PGE_2 modulates angiogenesis by augmenting the release of angiogenic peptides such as VEGF, bFGF and TGF-β.[8,9] We and others suggested that COX-2 inhibitors suppress tumor growth by inhibiting angiogenesis presumably an early phase of tumor development.[9,20,21] In the present advanced tumor model; however, celecoxib alone did not have a significant inhibitory effect on the growth of the established tumors, although celecoxib inhibited angiogenesis. Antiangiogenic effect of celecoxib alone may not be sufficient to suppress the growth of established tumors, because some tumor vessels may have already developed in the established tumors before treatment. 5FU also significantly inhibited tumor angiogenesis in the advanced colon 26 allografts in mice, suggesting that 5FU has an antiangiogenic effect in addition to the direct antitumor effects. Celecoxib enhanced the antitumor effect of 5FU, significantly inhibiting angiogenesis and tumor growth compared with animals treated with 5FU alone. The combination of 5FU and celecoxib exerted the most potent antiangiogenic effect as well as the most prominent antitumor effect to the established cancer allograft within the groups examined. These results suggest that the antiangiogenic effect of celecoxib enhances the antitumor effects of 5FU, although celecoxib alone is not sufficient to suppress the proliferation of established tumors.

VEGF is one of the most important angiogenic factors involved in tumor angiogenesis. In the present study, the combination of celecoxib and 5FU, 5FU alone and celecoxib alone decreased VEGF in tumor tissue. PGE_2 is reported to induce VEGF production *via* Akt and HIF activation.[22] How 5FU was able to reduce VEGF remains to be investigated in future studies.

5FU/celecoxib significantly increased IFN-γ levels, although no significant difference in IL-10 or IL-12 was noted among the treatment groups. To investigate the role of the host-derived IFN-γ in the established tumors, the antitumor effects of 5FU/celecoxib were evaluated in IFN-$\gamma^{-/-}$ mice. Treatment with celecoxib and 5FU was less effective at reducing the tumor volume in the IFN-$\gamma^{-/-}$ mice than in wild type mice. The results suggest that host IFN-γ plays an important role in the growth inhibition induced by the combined agents. IFN-γ is a cytokine that plays an important roles both immunologically and nonimmunologically in tumor development.[23] IFN-γ is reported to inhibit angiogenesis through the induction of IFN-γ inducible protein 10 (IP-10).[24] Another report showed that IFN-γ induces apoptosis of endothelial cells resulting in an inhibition of angiogenesis.[25] In the present study, 5FU/celecoxib significantly inhibited angiogenesis compared with 5FU alone, although both treatments significantly decreased tumor VEGF production. On the other hand, 5FU/celecoxib increased IFN-γ levels, whereas 5FU showed no effect on IFN-γ level in the tumors. One may hypothesize that the inhibition of angiogenesis is also related to elevation in tumor IFN-γ levels. To examine this hypothesis, the effect of celecoxib and 5FU on tumor angiogenesis was investigated using the IFN-$\gamma^{-/-}$ mouse model. The absence of IFN-γ significantly impaired the antiangiogenic effect of 5FU/celecoxib combination therapy. Consequently, IFN-γ, induced by the 5FU/celecoxib, has significant impact in suppressing angiogenesis and tumor growth.

Direct influences of celecoxib and 5FU on tumor cells should also be considered, although their distribution within the tumor *in vivo* might be difficult to extrapolate to cultured tumor cells *in vitro*. Our preliminary results indicate that 5FU (ranging from 0.4 to 20 μM) but not celecoxib (5–20 μM) reduce proliferation and viability in colon26 cells *in vitro*, unless the cells were seeded at an extremely-low density. Recent studies suggest that celecoxib and valdecoxib are able to inhibit carbonic anhydrase,[26,27] which may be a part of anticancer properties of the compounds both *in vitro* and *in vivo*. A study found that celecoxib, but not rofecoxib, inhibited growth of hematopoietic and epithelial cell lines that do not express COX-2.[28] This new property of celecoxib against cancer should be examined using a panel of COX-2 inhibitors *in vivo* and *in vitro*. However, this is not the case for colon26, to which celecoxib does not exert anticancer properties *in vitro*.

In conclusion, the combination of celecoxib and 5FU synergistically suppresses the growth of colon cancer allografts that have already grown in mice. Celecoxib in combination with 5FU suppresses tumor vasculature *via* inhibiting VEGF and elevating IFN-γ in the tumors. Although VEGF is another mediator as shown and discussed, the analyses using IFN-$\gamma^{-/-}$ mice demonstrate that IFN-γ is one of the crucial mediators of these phenomena. Thus, celecoxib treatment in combination with 5-FU-related chemotherapy will be a promising therapeutic strategy for the treatment of advanced colorectal adenocarcinomas.

References

1. Giovannucci E, Egan KM, Hunter DJ, Stampfer MJ, Colditz GA, Willett WC, Speizer FE. Aspirin and the risk of colorectal cancer in women. N Engl J Med 1995;333:609–14.
2. Tsujii M, DuBois RN. Alterations in cellular adhesion and apoptosis in epithelial cells overexpressing prostaglandin endoperoxide synthase 2. Cell 1995;83:493–501.
3. Tsujii M, Kawano S, DuBois RN. Cyclooxygenase-2 expression in human colon cancer cells increases metastatic potential. Proc Natl Acad Sci USA 1997;94:3336–40.
4. Boolbol SK, Dannenberg AJ, Chadburn A, Martucci C, Guo XJ, Ramonetti JT, Abreu-Goris M, Newmark HL, Lipkin ML, DeCosse JJ, Bertagnolli MM. Cyclooxygenase-2 overexpression and tumor formation are blocked by sulindac in a murine model of familial adenomatous polyposis. Cancer Res 1996;56:2556–60.
5. Pai R, Soreghan B, Szabo IL, Pavelka M, Baatar D, Tarnawski AS. Prostaglandin E2 transactivates EGF receptor: a novel mechanism for promoting colon cancer growth and gastrointestinal hypertrophy. Nat Med 2002;8:289–93.
6. Yasumaru M, Tsuji S, Tsujii M, Irie T, Komori M, Kimura A, Nishida T, Kakiuchi Y, Kawai N, Murata H, Horimoto M, Sasaki Y et al. Inhibition of angiotensin II activity enhanced the antitumor effect of cyclooxygenase-2 inhibitors via insulin-like growth factor I receptor pathway. Cancer Res 2003;63:6726–34.
7. Tendo M, Yashiro M, Nakazawa K, Yamada N, Hirakawa K. Inhibitory effect of a selective cyclooxygenase inhibitor on the invasion-stimulating activity of orthotopic fibroblasts for scirrhous gastric cancer cells. Cancer Sci 2005;96:451–5.
8. Tsujii M, Kawano S, Tsuji S, Sawaoka H, Hori M, DuBois RN. Cyclooxygenase regulates angiogenesis induced by colon cancer cells. Cell 1998;93:705–16.
9. Sawaoka H, Tsuji S, Tsujii M, Gunawan ES, Sasaki Y, Kawano S, Hori M. Cyclooxygenase inhibitors suppress angiogenesis and reduce tumor growth in vivo. Lab Invest 1999;79:1469–77.
10. Yao M, Kargman S, Lam EC, Kelly CR, Zheng Y, Luk P, Kwong E, Evans JF, Wolfe MM. Inhibition of cyclooxygenase-2 by rofecoxib attenuates the growth and metastatic potential of colorectal carcinoma in mice. Cancer Res 2003;63:586–92.
11. Hida T, Kozaki K, Ito H, Miyaishi O, Tatematsu Y, Suzuki T, Matsuo K, Sugiura T, Ogawa M, Takahashi T. Significant growth inhibition of human lung cancer cells both in vitro and in vivo by the combined use of a selective cyclooxygenase 2 inhibitor, JTE-522, and conventional anticancer agents. Clin Cancer Res 2002;8:2443–7.
12. Lin E, Morris JS, Ayers GD. Effect of celecoxib on capecitabine-induced hand-foot syndrome and antitumor activity. Oncology (Williston Park) 2002;16:31–7.

13. Becerra CR, Frenkel EP, Ashfaq R, Gaynor RB. Increased toxicity and lack of efficacy of Rofecoxib in combination with chemotherapy for treatment of metastatic colorectal cancer: a phase II study. Int J Cancer 2003;105:868–72.
14. Blumenthal RD, Waskewich C, Goldenberg DM, Lew W, Flefleh C, Burton J. Chronotherapy and chronotoxicity of the cyclooxygenase-2 inhibitor, celecoxib, in athymic mice bearing human breast cancer xenografts. Clin Cancer Res 2001;7:3178–85.
15. Sohn KJ, Croxford R, Yates Z, Lucock M, Kim YI. Effect of the methylenetetrahydrofolate reductase C677T polymorphism on chemosensitivity of colon and breast cancer cells to 5-fluorouracil and methotrexate. J Natl Cancer Inst 2004;96:134–44.
16. Kralovanszky J, Katona C, Jeney A, Pandi E, Noordhuis P, Erdelyi-Toth V, Otvos L, Kovacs P, Van der Wilt CL, Peters GJ. 5-ethyl-2′-deoxyuridine, a modulator of both antitumour action and pharmacokinetics of 5-fluorouracil. J Cancer Res Clin Oncol 1999;125:675–84.
17. Corbett TH, Griswold DP Jr, Roberts BJ, Peckham JC, Schabel FM Jr. Evaluation of single agents and combinations of chemotherapeutic agents in mouse colon carcinomas. Cancer 1977;40:2660–80.
18. Irie T, Tsuji S, Tsujii M, Komori M, Nishida T, Kakiuchi Y, Yasumaru M, Kawai N, Iijima H, Murata H, Sasaki Y, Hayashi N et al. Effect of Non-Steroidal Anti-Inflammatory Drugs (NSAIDs) with 5-Fluorouracil in Colon Cancer. Gastroenterology A 2003;124: 57.
19. Folkman J. Anti-angiogenesis: new concept for therapy of solid tumors. Ann Surg 1972;175:409–16.
20. Masferrer JL, Leahy KM, Koki AT, Zweifel BS, Settle SL, Woerner BM, Edwards DA, Flickinger AG, Moore RJ, Seibert K. Antiangiogenic and antitumor activities of cyclooxygenase-2 inhibitors. Cancer Res 2000;60:1306–11.
21. Wu YL, Fu SL, Zhang YP, Qiao MM, Chen Y. Cyclooxygenase-2 inhibitors suppress angiogenesis and growth of gastric cancer xenografts. Biomed Pharmacother 2005;59(Suppl 2):S289–S292.
22. Fukuda R, Kelly B, Semenza GL. Vascular endothelial growth factor gene expression in colon cancer cells exposed to prostaglandin E2 is mediated by hypoxia-inducible factor 1. Cancer Res 2003;63:2330–4.
23. Ikeda H, Old LJ, Schreiber RD. The roles of IFN gamma in protection against tumor development and cancer immunoediting. Cytokine Growth Factor Rev 2002;13:95–109.
24. Angiolillo AL, Sgadari C, Taub DD, Liao F, Farber JM, Maheshwari S, Kleinman HK, Reaman GH, Tosato G. Human interferon-inducible protein 10 is a potent inhibitor of angiogenesis in vivo. J Exp Med 1995;182:155–62.
25. Ribatti D, Nico B, Pezzolo A, Vacca A, Meazza R, Cinti R, Carlini B, Parodi F, Pistoia V, Corrias MV. Angiogenesis in a human neuroblastoma xenograft model: mechanisms and inhibition by tumour-derived interferon-gamma. Br J Cancer 2006;94:1845–52.
26. Knudsen JF, Carlsson U, Hammarstrom P, Sokol GH, Cantilena LR. The cyclooxygenase-2 inhibitor celecoxib is a potent inhibitor of human carbonic anhydrase II. Inflammation 2004;28:285–90.
27. Weber A, Casini A, Heine A, Kuhn D, Supuran CT, Scozzafava A, Klebe G. Unexpected nanomolar inhibition of carbonic anhydrase by COX-2-selective celecoxib: new pharmacological opportunities due to related binding site recognition. J Med Chem 2004;47:550–7.
28. Waskewich C, Blumenthal RD, Li H, Stein R, Goldenberg DM, Burton J. Celecoxib exhibits the greatest potency amongst cyclooxygenase (COX) inhibitors for growth inhibition of COX-2-negative hematopoietic and epithelial cell lines. Cancer Res 2002;62:2029–33.

Immunotherapy of Murine Colon Cancer Using Receptor Tyrosine Kinase EphA2-derived Peptide-pulsed Dendritic Cell Vaccines

Shinjiro Yamaguchi, MD[1]
Tomohide Tatsumi, MD, PhD[1,2]
Tetsuo Takehara, MD, PhD[1]
Ryotaro Sakamori, MD[1]
Akio Uemura, MD[1]
Tsunekazu Mizushima, MD, PhD[3]
Kazuyoshi Ohkawa, MD, PhD[1]
Walter J. Storkus, PhD[4,5]
Norio Hayashi, MD, PhD[1]

[1] Department of Gastroenterology and Hepatology, Osaka University Graduate School of Medicine, Osaka, Japan.

[2] Medical Center for Translational Research, Osaka University Hospital, Osaka, Japan.

[3] Department of Surgery, Rinku General Medical Center, Izumisano Municipal Hospital, Osaka, Japan.

[4] Department of Dermatology, University of Pittsburgh School of Medicine, Pittsburgh, Pennsylvania.

[5] Department of Immunology, University of Pittsburgh School of Medicine, Pittsburgh, Pennsylvania.

The first two authors contributed equally to this article.

Supported by a Grant-in-Aid from the Ministry of Education, Culture, Sports, Science, and Technology of Japan and by a Grant-in-Aid for Research on Hepatitis and Bovine Spongiform Encephalopathy from the Ministry of Health, Labor, and Welfare of Japan.

We thank Ms. Kyoko Iwase (Osaka University) for her excellent technical support.

Address for reprints: Norio Hayashi, MD, PhD, Department of Gastroenterology and Hepatology, Osaka University Graduate School of Medicine, 2-2 Yamadaoka, Suita, Osaka, 565-0871, Japan; Fax: (011) 81-6-6879-3629; E-mail: hayashin@gh.med.osaka-u.ac.jp

Received January 9, 2007; revision received May 8, 2007; accepted June 6, 2007.

BACKGROUND. Further optimization of dendritic cell (DC)-based vaccines is required clinically against advanced stage cancer. Given the broad range of expression levels observed in the recently defined tumor antigen EphA2 in a diverse types of cancers, especially in advanced stage or metastatic cancers, the authors evaluated the effectiveness of vaccination using DCs pulsed with EphA2-derived peptides (Eph-DCs) in a murine colon cancer model.

METHODS. EphA2 protein expression levels were evaluated in advanced colorectal carcinoma tissues from 10 patients by Western blot analysis. C57BL/6 mice were immunized with Eph-DCs twice weekly. Interferon γ (IFN-γ) ELISPOT assays were used for the analysis of CD8-positive T cells that were specific for EphA2-derived peptide. Immunized mice were challenged subcutaneously with EphA2-positive murine colorectal adenocarcinoma (MC38) mouse colon tumors or with EphA2-negative BL6 melanoma tumors. In some experiments, mice were injected with anti-CD8, anti-CD4, or antiasialo GM1 antibody to deplete corresponding lymphocyte subsets.

RESULTS. Among 10 samples of advanced colorectal carcinoma, 6 samples (60%) overexpressed EphA2. IFN-γ ELISPOT assays revealed that EphA2-derived peptide-specific CD8-positive T cells were generated by immunization with Eph-DCs. Immunization with Eph-DCs inhibited MC38 tumor growth compared with immunization using unpulsed DCs or phosphate-buffered saline. In contrast, Eph-DC vaccination had no effect on BL6 growth. Antibody depletion studies revealed that both CD8-positive T cells and CD4-positive T cells, but not natural killer cells, played critical roles in the efficacy observed for immunizations with Eph-DCs. Eph-DC vaccines resulted in long-term antitumor immunity against a rechallenge with MC38 tumor cells.

CONCLUSIONS. The current results demonstrated that Eph-DC vaccines may represent a promising preventative/therapeutic modality in the cancer setting. *Cancer* **2007;110:1469–77.** © *2007 American Cancer Society.*

KEYWORDS: dendritic cells, EphA2, colorectal cancer, cancer immunotherapy.

Dendritic cell (DC)-based vaccines are attractive cancer modalities, because DCs can induce both tumor antigen-specific cytotoxic T lymphocytes (CTLs) and helper-T cells. In this regard, DCs pulsed with tumor-associated antigens in various forms, including whole cell lysates,[1] proteins,[2] peptides,[3] RNA,[4] or DNA,[5] have been proven effective in eliciting protective and therapeutic antitumor immunity in murine models. The results of several DC-based tumor vaccine trials also recently have been reported for patients who had late-stage B-cell lymphoma, melanoma, prostate cancer, and renal

DOI 10.1002/cncr.22958
Published online 8 August 2007 in Wiley InterScience (www.interscience.wiley.com).

cell carcinoma.[6–9] In colorectal carcinomas, DC-based vaccines using synthetic peptides derived from known tumor antigens, such as carcinoembryonic antigen (CEA), also have been reported; however, to our knowledge to date, objective clinical responses have been observed only in a minority of treated patients with colon cancer.[10–12] Thus, a new strategy for tumor antigen-derived peptide-DC vaccines is expected to improve the clinical efficacy in patients with advanced colon cancer.

The Eph family constitutes the largest family of receptor tyrosine kinases, consisting of 2 Eph classes (EphA and EphB) and 2 classes of corresponding ligands, ephrin A and ephrin B, respectively. Because they are known largely for their role in neuronal development and tissue remodeling,[13–15] it has been suggested recently that Eph receptors play a role in oncogenesis[16–18] and tumor angiogenesis.[19,20] EphA2 is overexpressed in numerous cancer types, including melanoma[21] and prostate,[8] breast,[22] lung,[23] renal cell,[24] and colorectal[25] carcinomas; and it is altered functionally to promote the development of disseminated disease in a large number of different cancers. Indeed, the highest degree of EphA2 expression among tumors is observed most commonly in metastatic lesions, suggesting that EphA2 may represent a high-priority target for immunotherapy, especially in patients with advanced stage or metastatic cancer. We previously demonstrated that some patients with renal cell carcinoma exhibited both CD8-positive and CD4-positive T-cell responses to novel, EphA2-derived epitopes and that EphA2-derived epitopes were useful for predicting disease status and outcome as immunomonitoring targets.[26,27] These results also supported the therapeutic potential of EphA2 peptide-pulsed DC (Eph-DC)-based vaccines, although they have not been evaluated to date.

In the current study, we have demonstrated that vaccination with Eph-DCs elicits EphA2-specific CTL responses that are protective against EphA2-positive tumors, but not against EphA2-negative tumors. These results support the translational development of Eph-DC vaccines for patients with EphA2-positive colon cancer.

MATERIALS AND METHODS

Mice

Female C57BL/6 mice were purchased from Clea Japan, Inc. (Tokyo, Japan) and were used at ages 6 weeks to 8 weeks. They were housed under conditions of controlled temperature and light with free access to food and water at the Institute of Experimental Animal Science, Osaka University Graduate School of Medicine. All animals received humane care, and the study protocol complied with the institution's guidelines.

Cell Lines

MC38, a mouse colon carcinoma cell derived from C57BL6/J mice, was generously provided by Dr. Kazumasa Hiroishi (Showa University School of Medicine, Tokyo, Japan). BL6, a melanoma cell line, and YAC-1, a sensitive cell line to natural killer (NK) cells, were purchased from American Type Culture Collection (ATCC) (Rockville, Md). These cell lines were maintained in complete medium (CM) (RPMI medium supplemented with 10% fetal bovine serum, 100 U/mL, penicillin and 100 μg/mL streptomycin) at 37°C in 5% carbon dioxide.

Peptides

The protein sequences of mouse EphA2 were obtained from Genbank and were analyzed for H-2K^b binding motifs using BioInformatics and Molecular Analysis Section and a proteosomal cleavage site-prediction system. The H-2K^b-binding murine (m)EphA2$_{682\text{-}689}$ epitope (VVSKYKPM) was synthesized using an automated, solid-phase peptide synthesizer in the protein synthesis facility at the University of Pittsburgh Cancer Institute and was purified (to >95%) by using reverse-phase high-performance liquid chromotography.[28]

Western Blot Analyses

The proteins in samples from 10 patients with advanced colorectal carcinoma (stage III or IV) and the lysates from mouse tumor cell lines were separated by sodium dodecyl sulfate-polyacrylamide gel electrophoresis and were analyzed for expression of EphA2 using EphA2 monoclonal antibody (C20 Ab; Santa Cruz Biotechnology, Inc., Santa Cruz, Calif). Blots were imaged on Hyperfilm (Amersham Bioscience, Buckinghamshire, U.K.) after using horseradish peroxidase-conjugated goat-antirabbit immunoglobulin G (Bio-Rad, Hercules, Calif) and the Super Signal West Pico Luminol Enhance Solution kit (Pierce, Rockford, Ill). Expression of β-actin served as a loading control.

Generation of DCs From Bone Marrow and DC-based Peptide Vaccines

With minor modifications, the procedure that we used in this study was described previously.[29] Briefly, C57BL/6 bone marrow cells were cultured in CM supplemented with 500 U/mL of recombinant murine granulocyte–macrophage-colony-stimulating factor (R&D Systems Inc., Minneapolis, Minn) and recombinant interleukin 4 (IL-4) (R&D Systems Inc.) for 9 days. DCs were separated by magnetic cell sorting

using CD11c microbeads (Miltenyi Biotec GmbH, Bergisch Gladbach, Germany) and typically represented >90% of the harvested population of cells based on morphology and expression of the CD40, CD80, CD86, and major histocompatibility (MHC) Class II cells (data not shown). DCs were incubated with mouse $Eph_{682-689}$ peptide at a concentration of 10 μg/mL per 10^6 DC/mL CM for 2 hours at 37 °C. The cells were harvested and washed 3 times with phosphate-buffered saline (PBS) before use.[30]

IFN-γ ELISPOT Assays for Peptide-reactive CD8-positive T-cell Response

Splenocytes were harvested 5 days after subcutaneous immunization with 1×10^6 Eph-DCs twice over a 1-week interval. CD8-positive T cells were isolated selectively from splenocytes by magnetic cell sorting using CD8 microbeads (Miltenyi Biotec). Mouse IFN-γ ELISPOT assays were performed using a mouse IFN-γ ELISPOT kit (R&D Systems Inc.) according to the manufacture's instructions. IFN-γ-secreting cells appeared as blue spots. The data are represented as the mean number (±standard deviation [SD]) of IFN-γ spots per 100,000 CD8-positive T cells analyzed.

Animal Experiments

C57BL/6 mice were immunized subcutaneously into the left flank with 1×10^6 Eph-DCs or unpulsed DCs in a total volume of 100 μL of PBS twice a week. On Day 0, for the second Eph-DC immunization, 2×10^5 MC38 cells as Eph A2-positive cells or 5×10^4 BL6 cells as EphA2-negative cells were injected subcutaneously into the right flank. To assess the impact of systemic immunity from subcutaneous injection of Eph-DCs, tumor size was assessed every week and was recorded in mm^2 by determining the product of the greatest perpendicular dimensions measured by Vernier calipers. Data are reported as the average tumor area ±SD.

Cytolytic Assay

Splenocytes were harvested 14 days after tumor inoculation. Responder cells (5×10^6 per well) were restimulated in vitro with 1×10^6 MC38 cells that had been treated with 0.5 mg/mL mitomycin C (Kyowa-Hakko, Tokyo, Japan) in the presence of 30 IU/mL recombinant murine IL-2 (Strathmann Biotech, Hannover, Germany). After 5 days of in vitro restimulation, lymphocytes were subjected to 4-hour ^{51}Cr release assays against the MC38 or BL6 targets, as described previously.[29] CD4-positive and CD8-positive T cells were depleted selectively from whole splenocytes by magnetic cell sorting using CD4 and CD8 microbeads (Miltenyi Biotec), respectively. In some experiments, splenocytes were harvested 1 day after tumor inoculation and were subjected directly to 4-hour ^{51}Cr release assays against YAC-1 targets (NK cell-sensitive cells).

T-Cell and NK Cell In Vivo Depletion Experiments

To deplete T cells in vivo, anti-CD4 (GK1.5 hybridoma; ATCC) or anti-CD8 antibody (53–6.72 hybridoma; ATCC) were administered intraperitoneally 4 days and 1 day before every tumor inoculation and then every 5 days after tumor inoculation. For depletion of NK cells in vivo, we used antiasialo GM1 antibody (Wako, Osaka, Japan), which was administered intraperitoneally 1 day before tumor inoculation and then every 5 days after tumor inoculation. The efficiency of specific subset depletions was validated by flow cytometry analysis of splenocytes. In all samples, 99% of the targeted cell subset was depleted specifically (data not shown).

Tumor Rechallenge

C57BL/6 mice were immunized subcutaneously with 1×10^6 Eph-DCs twice weekly and were challenged subcutaneously with 2×10^5 MC38 cells at the second Eph-DC immunization. Forty-two days after tumor inoculation, 2×10^5 MC38 cells were injected subcutaneously into the contralateral flank of the initial MC38 tumor on Day 0. For control experiments, 2×10^5 MC38 cells were injected subcutaneously into naive C57BL/6 mice on Day 0, at the same time of MC38 rechallenge. Tumor size was assessed every week after the second tumor inoculation.

Statistical Analyses

The statistical significance of differences between the groups was determined by applying a Student t test with Welch correction or a 1-way analysis of variance after each group had been tested with equal variance and Fisher exact probability test. Statistical significance was defined as $P < .05$.

RESULTS

Expression of EphA2 in Human Colorectal Cancer Tissues and Murine Tumor Cells

We evaluated the expression of EphA2 in samples from 10 patients with colorectal carcinoma and H-2^b-syngeneic murine tumor cell lines from C57BL/6 mice by Western blot analysis using a species cross-reactive monoclonal antibody. Figure 1A shows that 6 samples (60%) of advanced-stage disease (stage III or IV) overexpressed EphA2 compared with normal colon tissues. In addition, the murine colon cancer

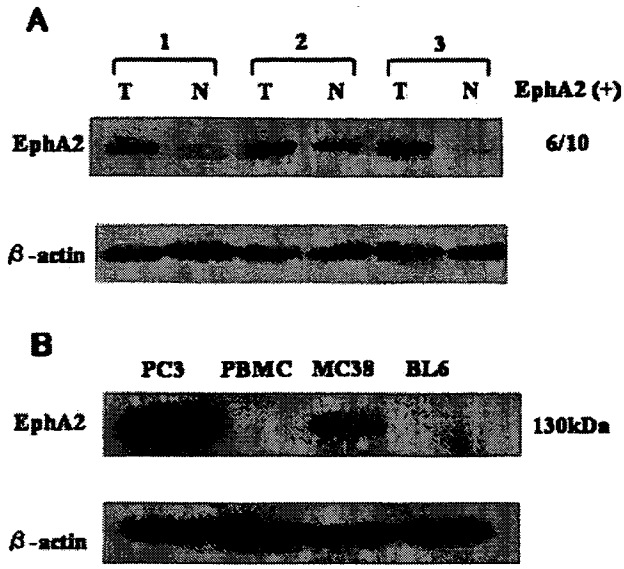

FIGURE 1. The expression levels of murine Eph receptor A2 (mEphA2) in human colorectal cancer tissues and murine tumor cells. The proteins in samples from 10 patients with colorectal carcinoma and the lysates of the murine colorectal adenocarcinoma (MC38) cell line and the BL6 melanoma cell line were evaluated for EphA2 protein expression by Western blot analysis, as described in the text. (A) Six samples (60%) of 10 advanced-stage samples (stage III or IV) expressed EphA2 protein compared with normal colon tissues. T and N indicate colon cancer tissue and its surrounding normal colon tissue, respectively. (B) The murine colon cancer cells (MC38) expressed EphA2 protein, but the murine melanoma cell line (BL6) did not. The human prostate cancer cell line PC3 was used as a positive control, and human peripheral blood mononuclear cells (PBMC) were used as a negative control. The expression of β-actin served as a loading control. KDa indicates kilodaltons.

cell line (MC38) expressed EphA2 protein, but the murine melanoma cell line (BL6) did not (Fig. 1B).

Detection of EphA2-derived Peptide-specific CD8-positive T Cells Secreting IFN-γ After Vaccination With Eph-DCs

We performed IFN-γ ELISPOT assays to examine whether subcutaneous injection of Eph-DCs could generate CD8-positive T cells that were specific for EphA2-derived peptide in vivo. Figure 2 shows that the frequency of specific CD8-positive T cells secreting IFN-γ in mice treated with Eph-DCs was significantly higher than the frequency observed in naive mice or in mice treated with unpulsed DCs. These results demonstrate that EphA2-specific, type 1, CD8-positive T cells effectively are generated by in vivo immunization with Eph-DCs.

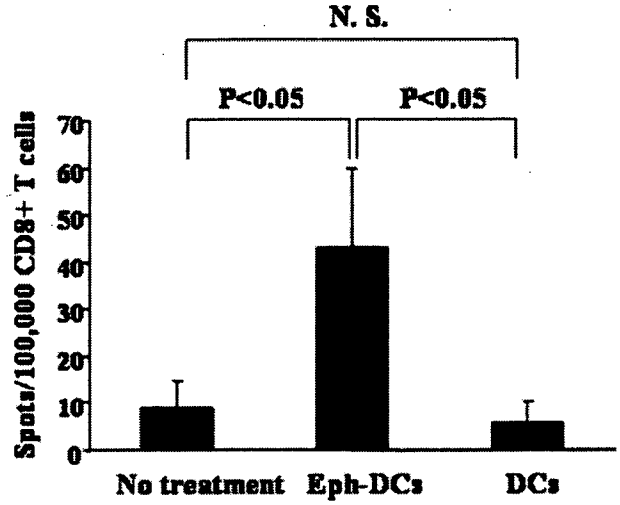

FIGURE 2. Interferon γ (IFN-γ) ELISPOT assays for peptide-reactive, CD8-positive T cell responses. Mice were vaccinated with the indicated agent and were killed on Day 5 after immunization. CD8-positive T cells were isolated form splenocytes using CD8 microbeads and then were subjected to IFN-γ ELISPOT assays to detect Eph receptor A2 (EphA2)-derived peptide-specific cytotoxic T lymphocytes (CTLs). The data are represented as the mean number (± standard deviation) of IFN-γ spots per 100,000 CD8-positive T cells analyzed. Similar results were obtained in 3 experiments. N.S. indicates not significant; Eph-DCs, Eph peptide-pulsed dendritic cells; DCs, dendritic cells.

Immunization With Eph-DCs Prevents Progression of EphA2-positive Tumors, but Not EphA2-negative Tumors, In Vivo

Next, we examined whether immunization with Eph-DCs (on Days −7 and 0) would induce protective antitumor effects against EphA2-positive MC38 colon cancer. Figure 3A shows that MC38 tumor growth in mice that were immunized with Eph-DCs was inhibited strongly compared with tumor growth in mice that were immunized with unpulsed DCs ($P < .05$ on Days 21 and 28) or with PBS ($P < .05$ on Days 14, 21, and 28), whereas tumor growth in mice that were immunized with unpulsed DCs was inhibited slightly compared with tumor growth in mice that received PBS ($P < .05$ on Days 21 and 28). Conversely, in vivo growth of EphA2-negative BL6 tumors in mice that were immunized with Eph-DCs or unpulsed DCs was inhibited slightly compared with the tumor growth in mice that received PBS ($P < .05$ on Day 28). However, it is noteworthy that there was no significant difference in BL6 tumor growth between the Eph-DC group and the unpulsed DC group (Fig. 3B). These results indicate that vaccination with Eph-DCs provides specific antitumor effects against relevant EphA2-positive MC38 tumors.

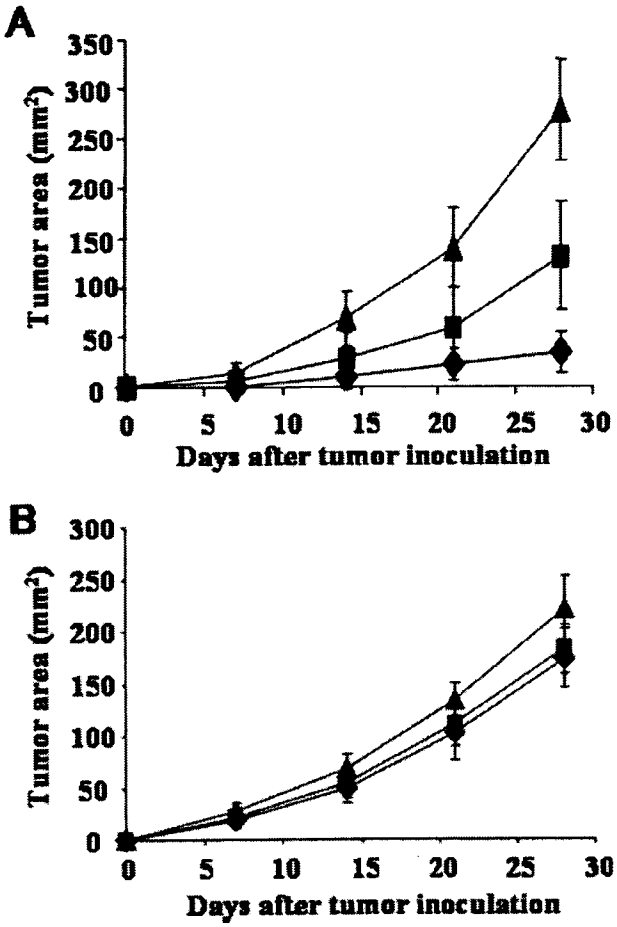

FIGURE 3. The antitumor effects of vaccination with EphA2-derived peptide-pulsed dendritic cells (Eph-DCs). C57BL/6 mice were immunized on Days −7 and 0 with 1×10^6 Eph-DCs (diamonds), unpulsed DCs (squares), or phosphate-buffered saline (PBS) (triangles). On Day 0, 2×10^5 murine colorectal adenocarcinoma (MC38) cells (A) or 5×10^4 BL6 melanoma cells (B) were injected subcutaneously. (A) MC38 tumor growth in mice that were immunized with Eph-DCs was inhibited significantly compared with tumor growth in mice treated on the other protocols ($P < .05$ on Days 14, 21, and 28 vs PBS; $P < .05$ on Days 21 and 28 vs unpulsed DCs). Tumor growth in mice that were immunized with unpulsed DCs was inhibited significantly compared with tumor growth in mice that received PBS on Days 21 and 28 ($P < .05$; N = 15 mice per group). (B) BL6 tumor growth in mice that were immunized with Eph-DCs or unpulsed DCs was inhibited compared with tumor growth in mice that received PBS ($P < .05$ on Day 28). Tumor growth in mice treated with Eph-DCs was not inhibited compared with mice treated with unpulsed DCs (N = 8 mice per group). Each data point represents the mean tumor size ±standard deviation.

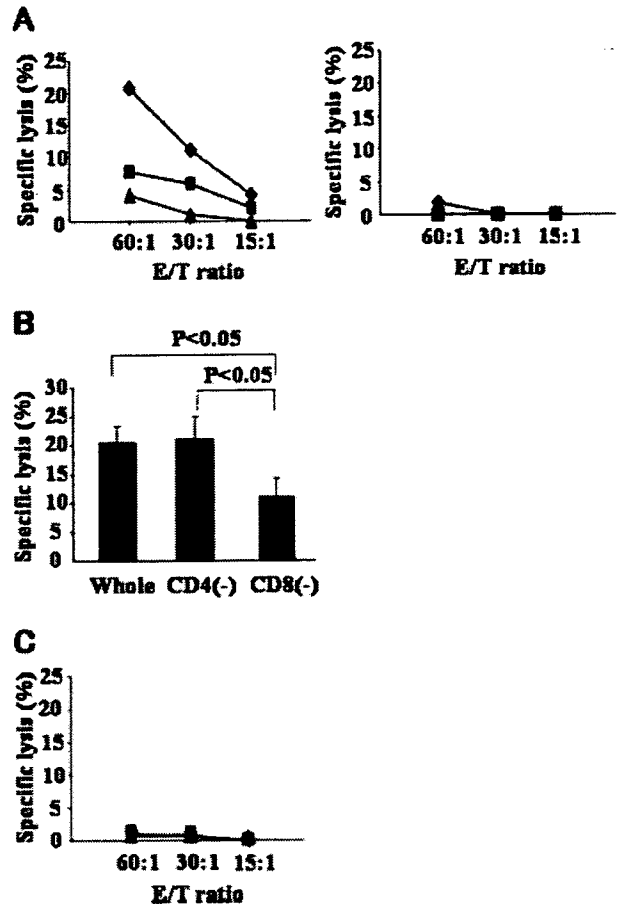

FIGURE 4. The induction of cytolytic activity by immunization with EphA2-derived peptide-pulsed dendritic cell (Eph-DC) vaccination. (A) Splenocytes were harvested from mice 14 days after final immunization with Eph-DCs (diamonds), unpulsed DCs (squares), or phosphate-buffered saline (PBS) (triangles) and tumor inoculation. Splenocytes were stimulated in vitro with mitomycin C-treated MC38 cells in the presence of recombinant human interleukin 2. After 5 days of culture, cytolytic activity was evaluated by 4-hour ^{51}Cr release cytolytic assays using MC38 cells (left) or BL6 cells (right) as targets at the indicated effector to target (E/T) ratios. (B) Before the 4-hour ^{51}Cr release cytolytic assays, whole splenocytes from Eph-DC-treated mice were depleted of CD4-positive or CD8-positive T cells by using CD4 or CD8 microbeads. Cytolytic activity against MC38 cells of depleted or nondepleted cells was compared (E/T ratio, 60:1). (C) Splenocytes were harvested 1 day after tumor inoculation. Without in vitro restimulation, whole splenocytes were subjected to 4-hour ^{51}Cr release assays against natural killer (NK)-sensitive YAC-1 cells as targets at the indicated E/T ratios. No cytolytic activity was observed against the NK-sensitive YAC-1 cells in any treatment arm (Eph-DCs [diamonds], unpulsed DCs [squares], PBS [triangles]). Similar results were obtained in 3 independent experiments (A-C).

Induction of Specific CTLs Against MC38 Cells After Immunization With Eph-DCs

For the next experiment, we examined whether our Eph-DC regimen could induce specific cytolytic reactivity against MC38 or BL6 cells. Splenocytes were harvested from the various treatment groups of mice that were killed 14 days after tumor inoculation. Figure 4A shows that splenocytes from mice treated with unpulsed DCs displayed weak cytolytic reactivity